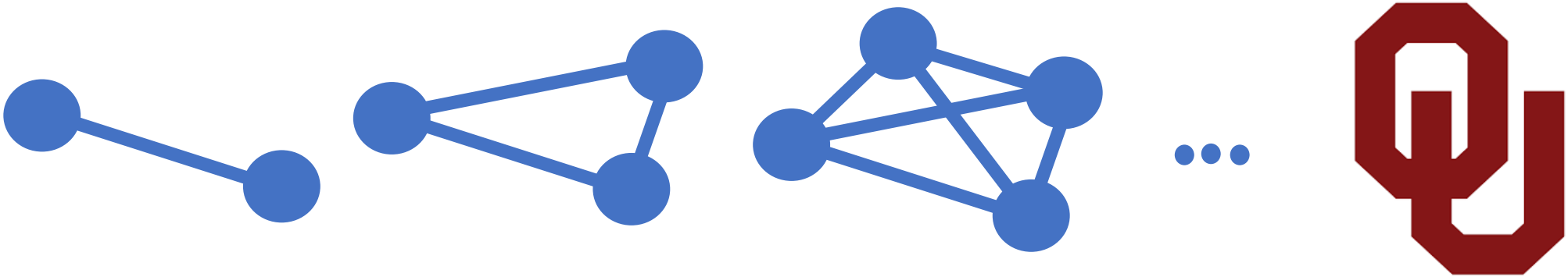

Small Atomic Quantum Systems with Large s-Wave Scattering Length

Doerte Blume
Center for Quantum Research and Technology (CQRT)
Department of Physics and Astronomy
The University of Oklahoma, Norman.

Collaborators over the years:
Marius Lewerenz, Peter J. Toennies, Birgitta K. Whaley,
Chris H. Greene, Brett Esry.
Gabriel Hanna, Yangqian Yan, Qingze Guan, AJ Yates,
Maksim Kunitski, Reinhard Doerner and group.

Supported by the NSF.

Helium Droplets: Cold But Not Ultracold Samples

Cold ^{4}He atoms (sub-Kelvin temperatures):

Three-body (three-body Efimov state)
Larger clusters
Two-body (real-time dynamics)

Size-selected nozzle beam expansion experiments

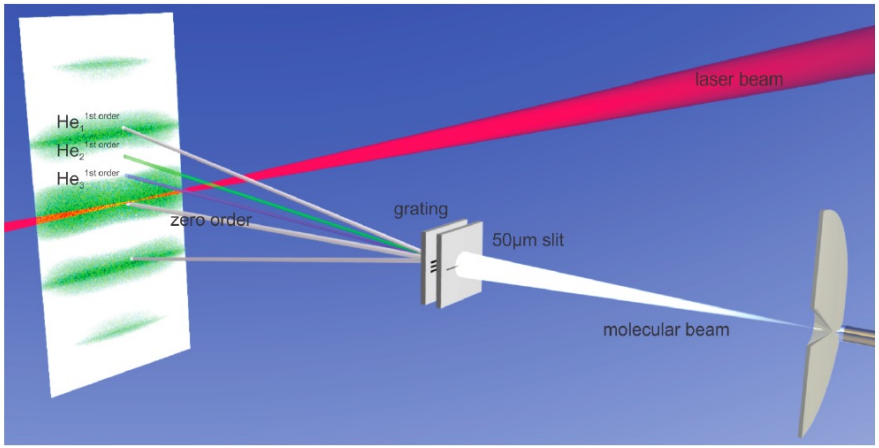

Superfluid Bulk Helium-4

- ^{4}He is the only substance that remains liquid under normal pressure at zero temperature (superfluid with condensate fraction of around 8%).
- Normal to superfluid transition at 2.17K.

Helium named after

the sun (greek “helios”).

Discovered in 1868.

Bulk liquid helium-4:

Binding energy per

particle E/N = −7K

(1 K = 8.6 x 10^{-5} eV).

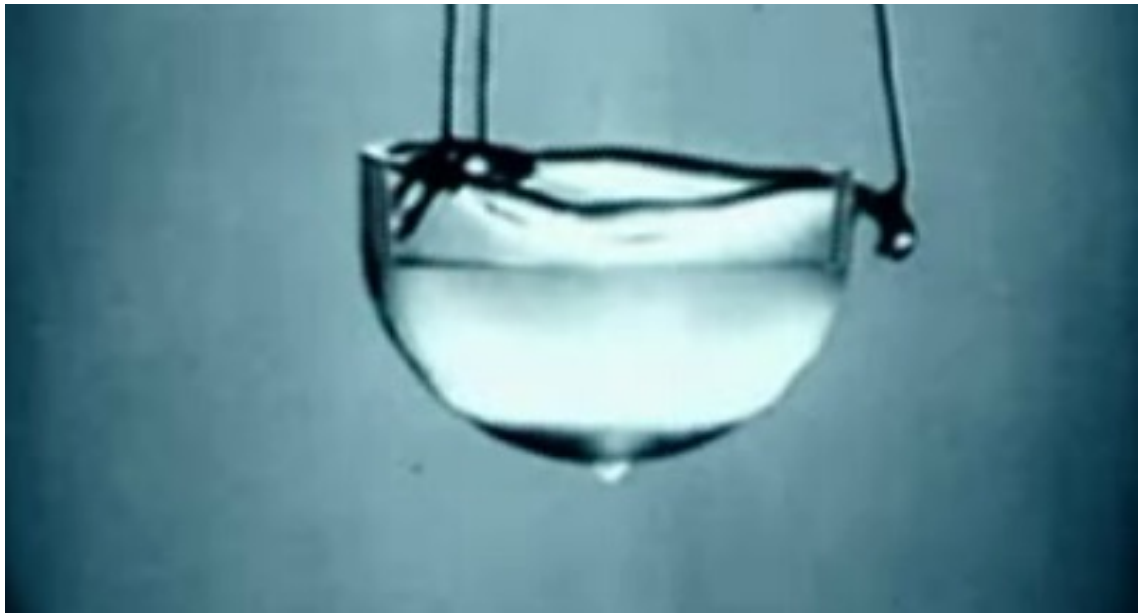

From Wikipedia

Helium Droplets = Quantum Liquid

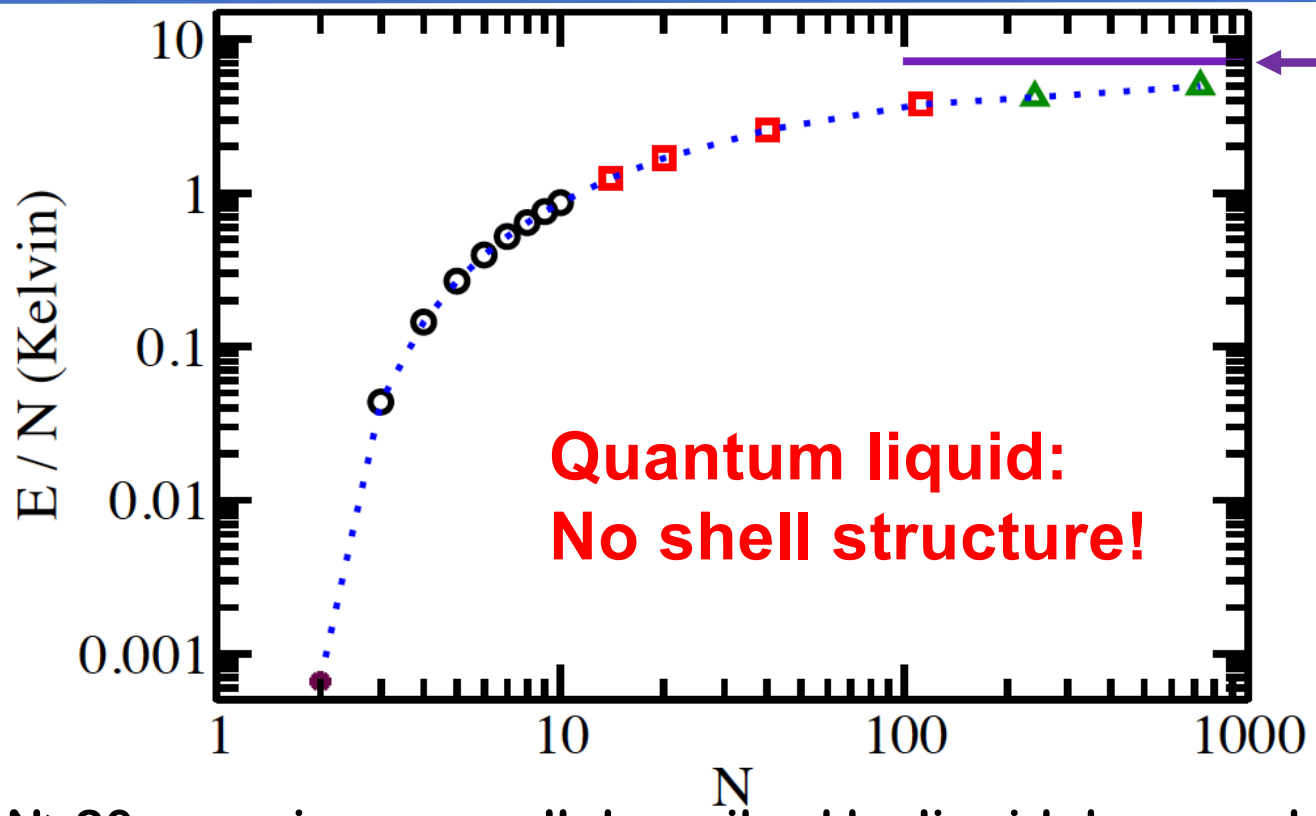

Large N: E/N ~ –7K

Well known literature results:

Small N (N<10): E/N ~ # N.

(E/N changes by four orders of magnitude.)

N>20 energies are well described by liquid drop model with volume and surface terms (no Coulomb, asymmetry, or pairing terms).

Rich interplay between many-body nuclear physics and quantum droplet community [e.g., Pandharipande et al., PRL 50, 1676 (1983); Stringari et al., JCP 87, 5021 (1987); Sindzingre et al., PRL 63, 1601 (1989)].

Helium Droplets: Matter Wave Diffraction Experiment

Kornilov, Toennies, 10.1051/epn:2007003

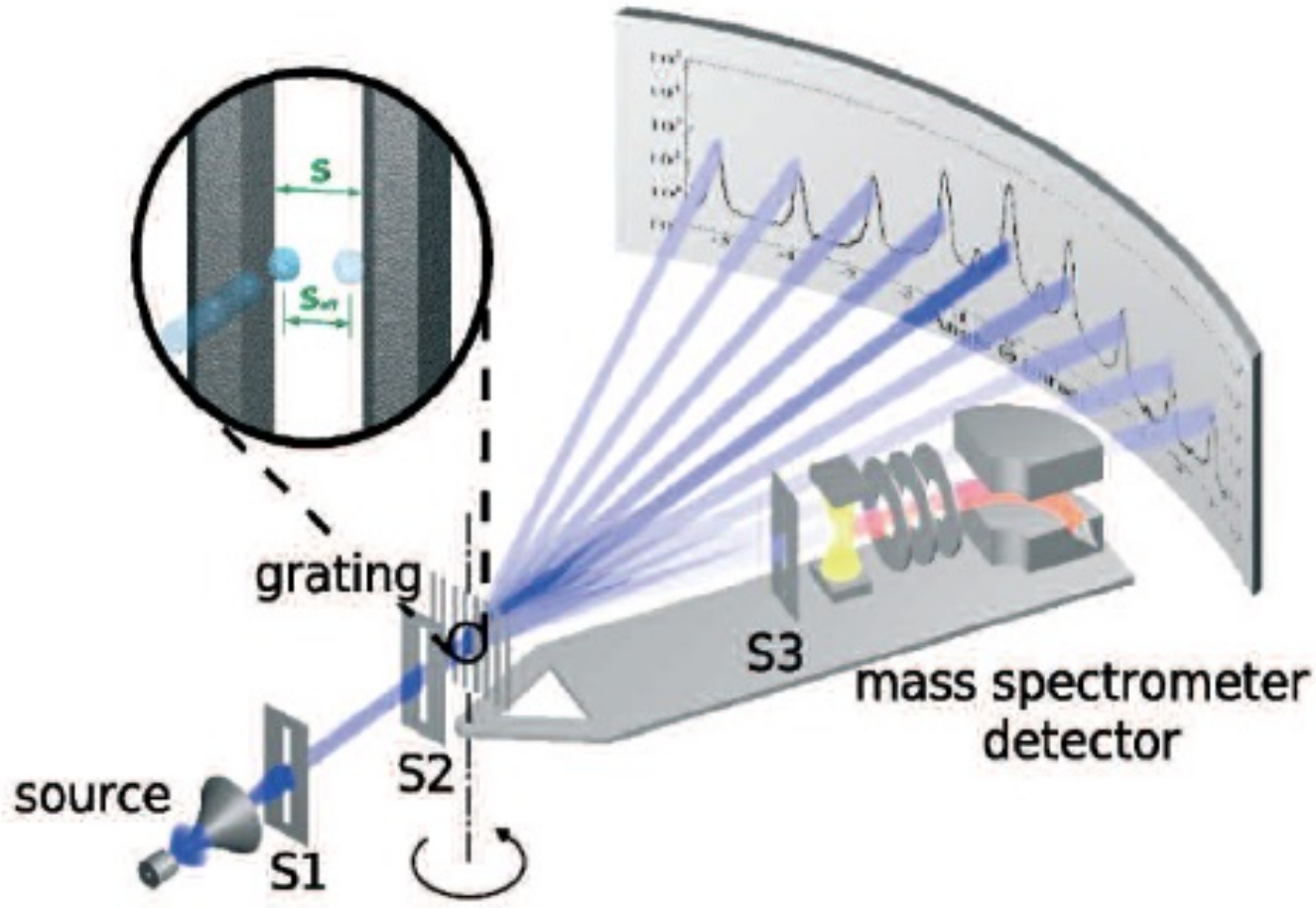

De Broglie wave length λ:

λ = h/(Mv)

Diffraction angle θ:

$$\sin\theta = n\frac{\lambda}{d} = n\frac{h}{N \cdot m \cdot v \cdot d}$$

v: velocity

n: diffraction order

m: mass of helium atom

N: number of helium Atoms

Nm: mass of cluster

Observation of Bosonic Helium Dimer: $^4He_2$

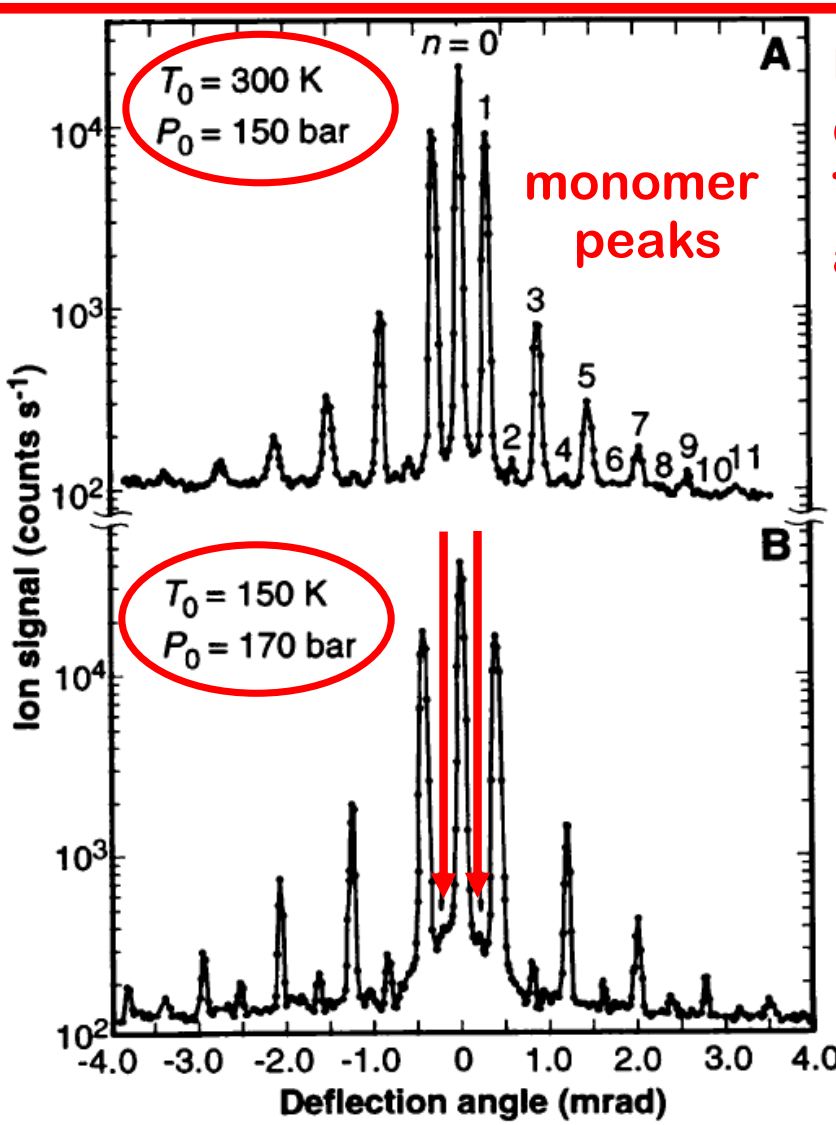

Fragile helium dimer forms in beam and can be isolated. Schoellkopf and Toennies, Science 266, 1345 (1994); see also Luo et al., JCP 98, 3564 (1993).

Nozzle temperature and pressure can be adjusted. Kornilov, Toennies, 10.1051/epn:2007003

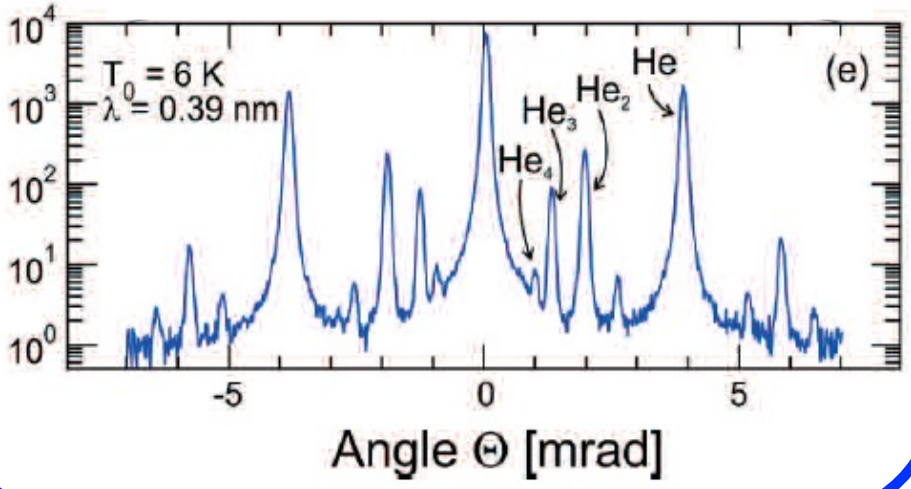

Debate on Helium Dimer

creasing with each passing year. When a recent PhD in a physical science said that helium formed diatomic molecules, I knew we were in trouble!

hat would be, let's see, 16 years ago now. Schöllkopf and Toennies diffracted helium atoms and dimers from a manmade transmission diffraction grating to show, beyond the shadow of a doubt, that the neutral helium dimer exists as a stable diatomic species (albeit extremely weakly bound). Given the highly quantum mechanical nature of this extraordinary dimer and the fact that it has perhaps the most weakly bound ground state of any dimer, it is of considerable fundamental interest.

R. Bruce Doak, Physics Today 65(8), 10 (2012)

Helium Dimer and Trimers

$1\ \mathrm{K} = 8.6 \times 10^{-5}\ \mathrm{eV}$

- Dimer:
  - ^{4}He-^{4}He bound state energy $E_{dimer} = -1.625$mK. No $J > 0$ bound states. ^{4}He-^{3}He does not support bound state.
  - Two-body s-wave scattering length $a_s = 170.86a_0$.
  - Two-body effective range $r_{eff} = 15.2a_0$
    (alternatively, two-body van der Waals length $r_{vdW} = 5.1a_0$).

- Trimer:
  - Two $J = 0$ bound states with $E_{trimer} = -131.8$mK and -2.65mK.
  - No $J > 0$ bound states.

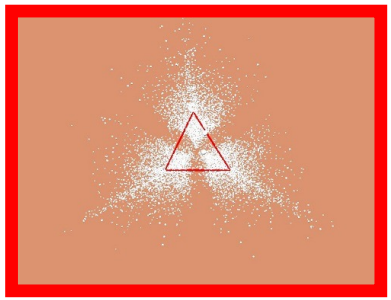

$(^4He_3)^*$

Discussed later in this talk.

Helium Dimer and Trimers

$1\ \mathrm{K} = 8.6 \times 10^{-5}\ \mathrm{eV}$

- Dimer:
  - ^{4}He-^{4}He bound state energy $E_{dimer} = -1.625$mK. No J > 0 bound states. ^{4}He-^{3}He does not support bound state.
  - Two-body s-wave scattering length $a_s = 170.86a_0$.
  - Two-body effective range $r_{eff} = 15.2a_0$
    (alternatively, two-body van der Waals length $r_{vdW} = 5.1a_0$).
- Trimer:
  - Two J = 0 bound states with $E_{trimer} = -1$3 -2.65mK.
  - No J > 0 bound states.

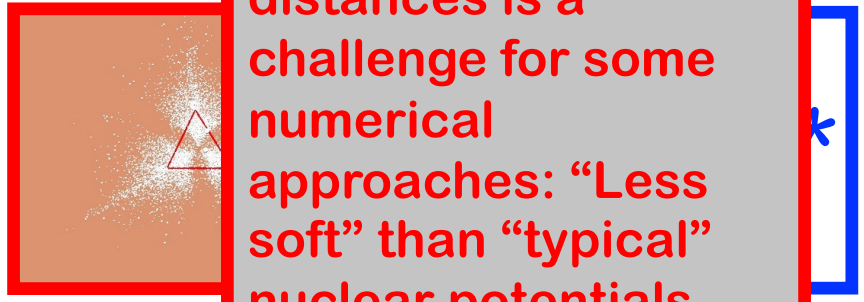

Close to hard wall at small internuclear distances is a challenge for some numerical approaches: "Less soft" than "typical" nuclear potentials.

- Nuclear physics: Deuteron and triton.

in this talk.

Comparison With Other Neutral Rare Gas Clusters

- ^{4}He, ^{10}Ne, ^{20}Ar: composite bosons (energy scales are such that these atoms can be considered as point particles; consider only nuclear degrees of freedom).

- Dimer (potential minimum at 5–10a_0):
  - ^{4}He-^{4}He binding energy: E_{dimer} = –1.3mK.
  - ^{10}Ne-^{10}Ne binding energy: E_{dimer} = –20.1K.
  - ^{20}Ar-^{20}Ar binding energy: E_{dimer} = –101K.

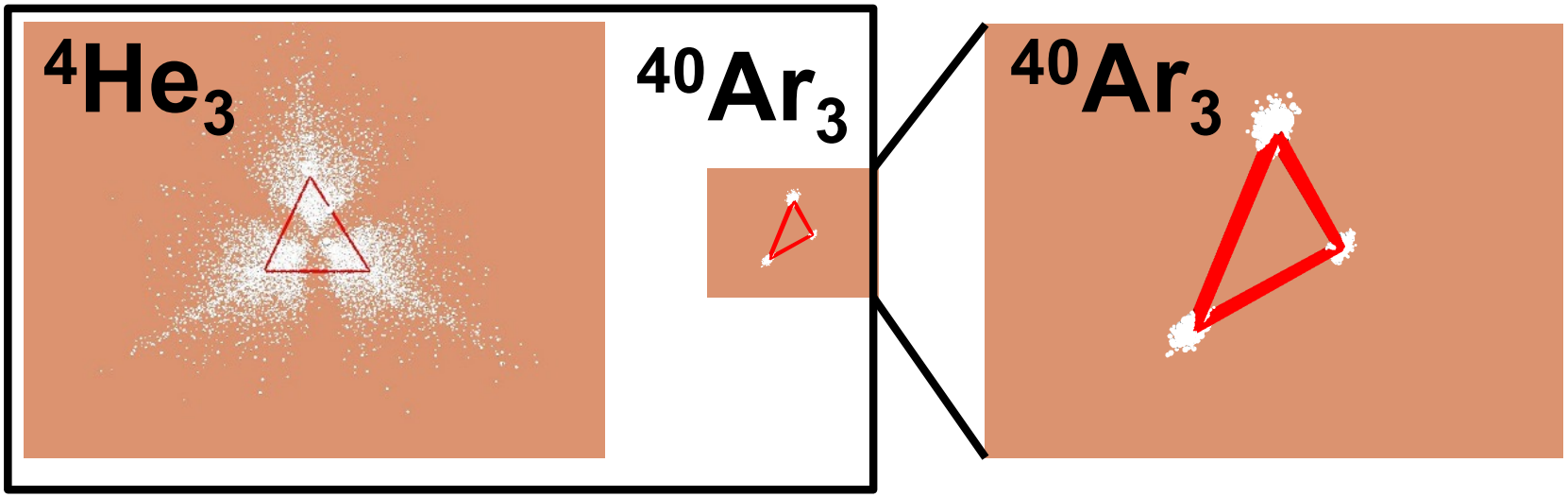

Helium Dimer

1 K = 8.6 x 10^{-5} eV

- Using modern Born-Oppenheimer potential:
  - ^{4}He-^{4}He bound state energy $E_{dimer} = -1.625\ \mathrm{mK}$.
  - Two-body s-wave scattering length $a_s = 170.86\ \mathrm{a_0}$.

- **Question: Is the ^{4}He dimer universal?**

  - $E_{dimer} = -5.147 \cdot 10^{-9}\ \mathrm{a.u.}$

  - Zero-range theory: $E_{dimer} = -\frac{\hbar^2}{m\, a_s^2} = -4.69 \cdot 10^{-9}\ \mathrm{a.u.}$ (≈91%)
  - Including effective range correction ($r_{eff} = 15.2\ \mathrm{a_0}$):

$$E_{dimer} = -\frac{\hbar^2}{m\, r_{eff}^2}\left(1 - \sqrt{1 - \frac{2r_{eff}}{a_s}}\right)^2 = -5.17 \cdot 10^{-9}\ \mathrm{a.u.}\ (\approx 100\%)$$

Visualizing the Difference

- Using modern Born-Oppenheimer potential:
  - ^{4}He-^{4}He bound state energy $E_{dimer} = -1.625\ \mathrm{mK}$.
  - Two-body s-wave scattering length $a_s = 170.86\ \mathrm{a_0}$.
  - Zero-range theory: probability $= \frac{2}{a_s} \exp\left(-2\frac{r}{a_s}\right)$.

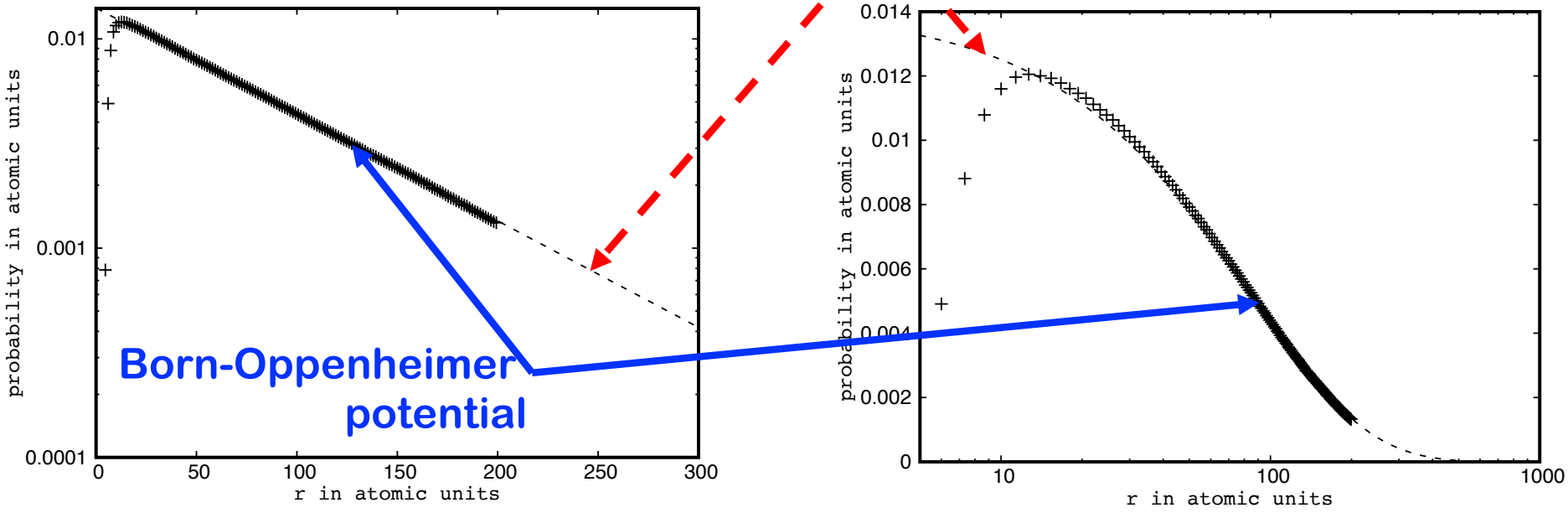

Visualizing The Difference

- Using modern Born-Oppenheimer potential:
  - ^{4}He-^{4}He bound state energy $E_{dimer} = -1.625\ \mathrm{mK}$.
  - Two-body s-wave scattering length $a_s = 170.86\ \mathrm{a_0}$.
  - Zero-range theory: probability $= \frac{2}{a_s} \exp\left(-2\frac{r}{a_s}\right)$.

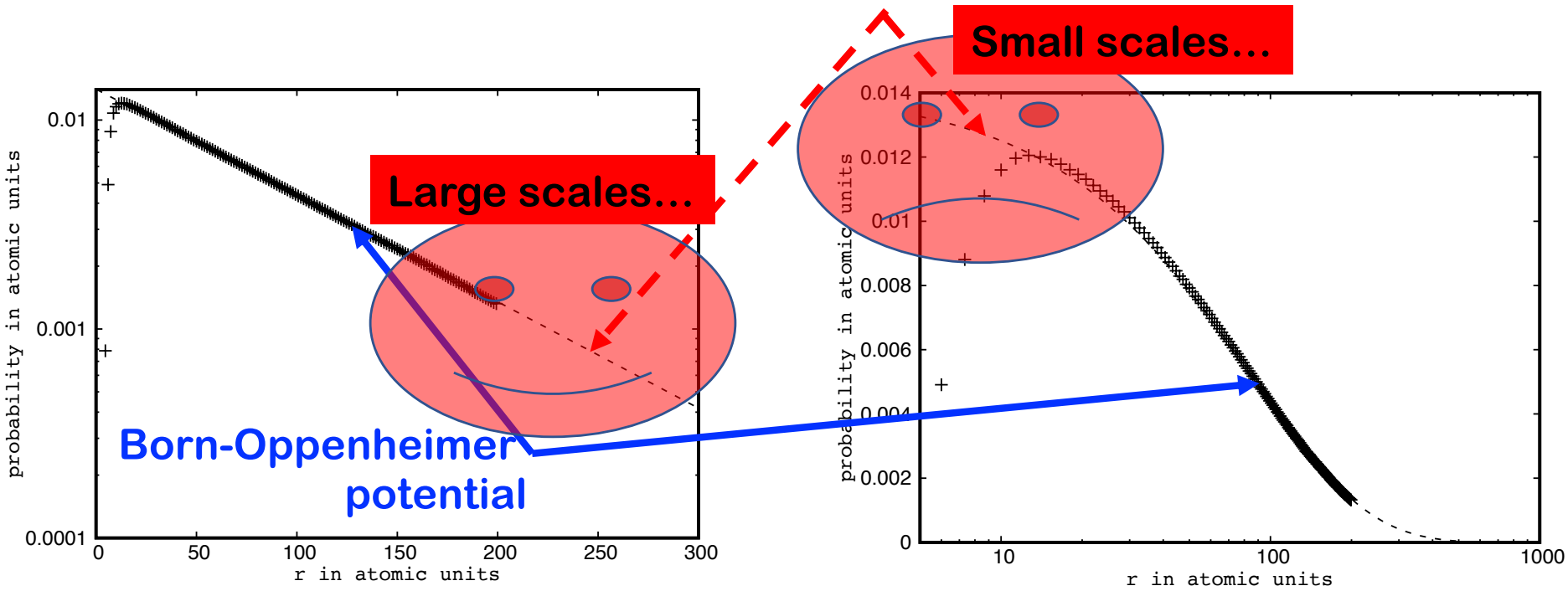

Comparison: Helium Dimer and Trimers

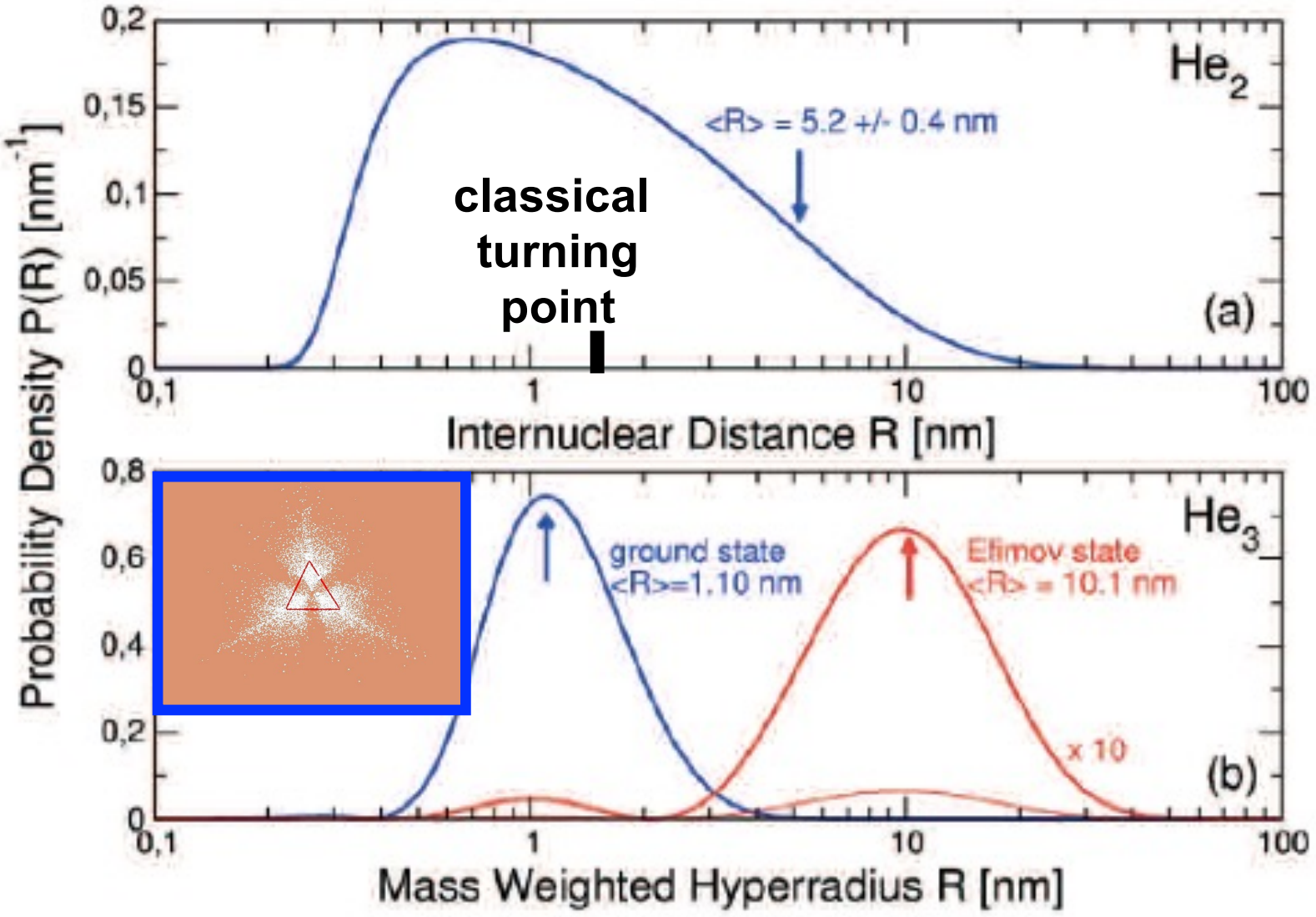

Kornilov, Toennies, 10.1051/epn: 2007003

Finite s-wave Scattering Length: Universally Linked States

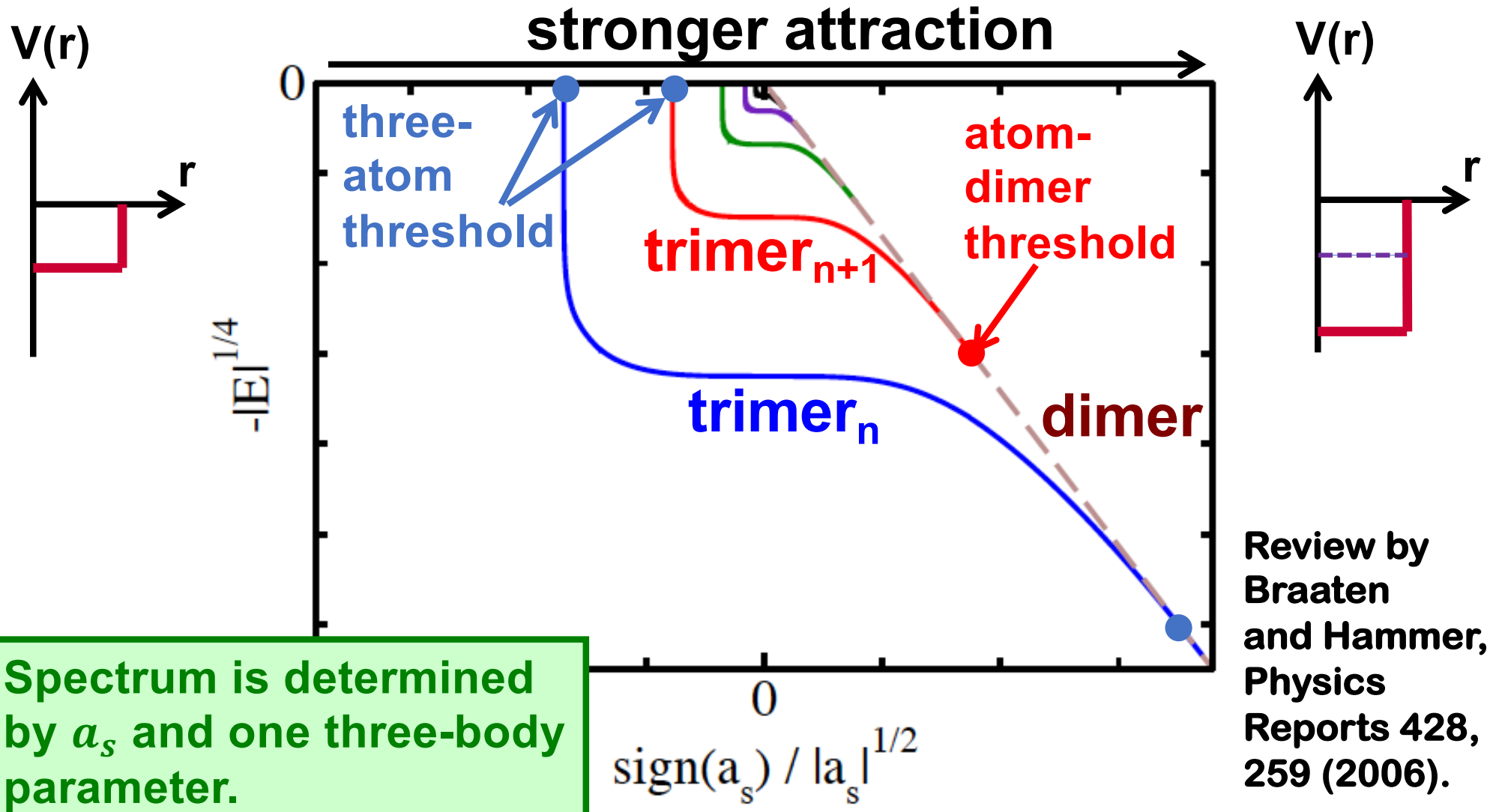

Spectrum is determined by a_s and one three-body parameter.

Review by Braaten and Hammer, Physics Reports 428, 259 (2006).

Helium Trimer Excited State is an Efimov State

$\beta V_{He\text{-}He}(r_{12}) + \beta V_{He\text{-}He}(r_{23}) + \beta V_{He\text{-}He}(r_{31})$.

Three-body parameter is chosen such that ZR energy agrees with energy of scaled helium trimer excited state.

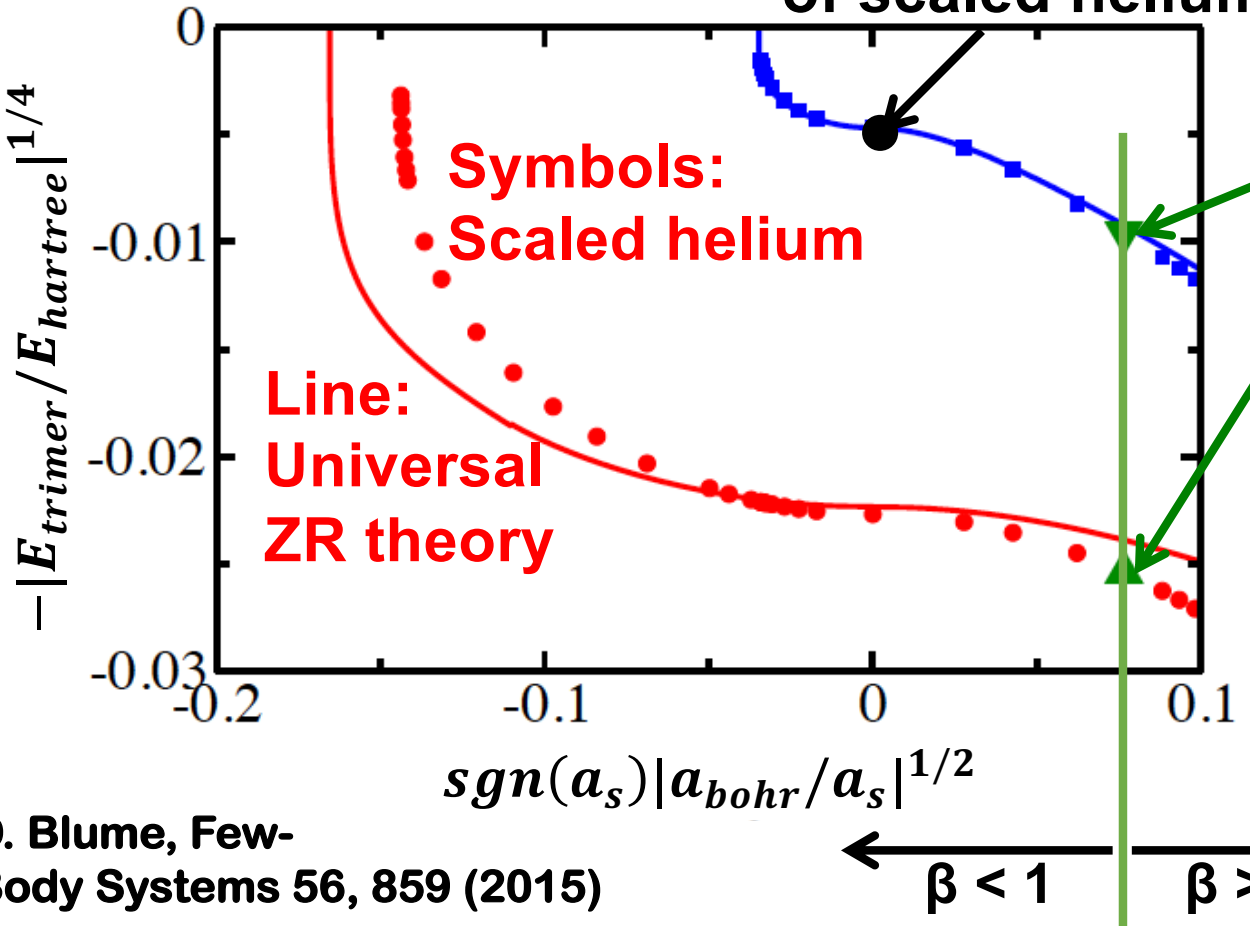

True helium (ground and excited states)

For the excited state, symbols agree with line! Molecular system follows predicted Efimov behavior.

D. Blume, Few-Body Systems 56, 859 (2015)

Probing Helium Trimer Excited Efimov State

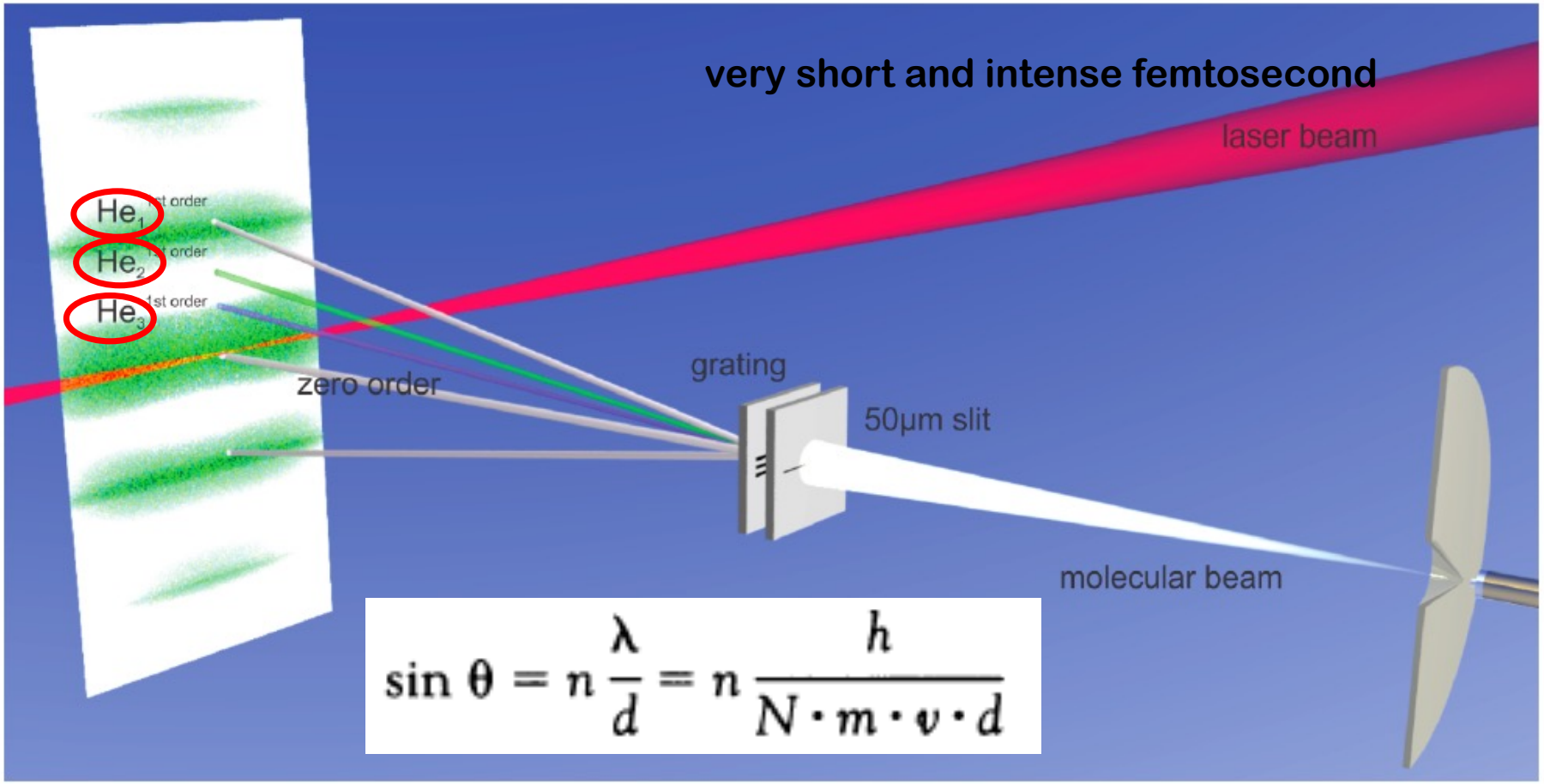

Probing Helium Trimer Excited Efimov State

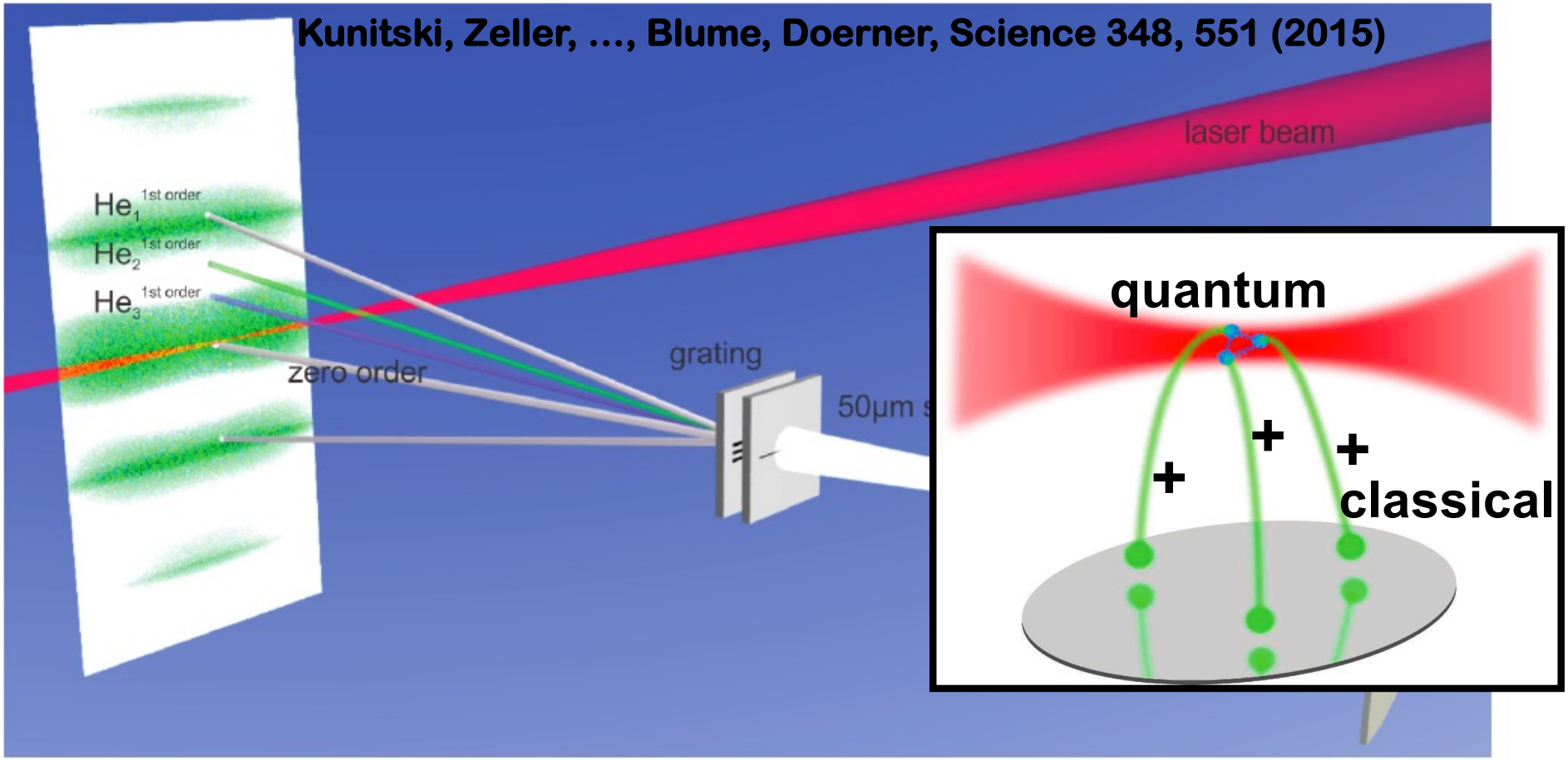

He_3 signal contains ground state trimer *and* excited state trimer.
Laser beam ionizes trimer: Coulomb explosion of $^4He_3$ (3 ions).

Kinetic Energy Release Measurement: Observing $(^4He_3)^*$

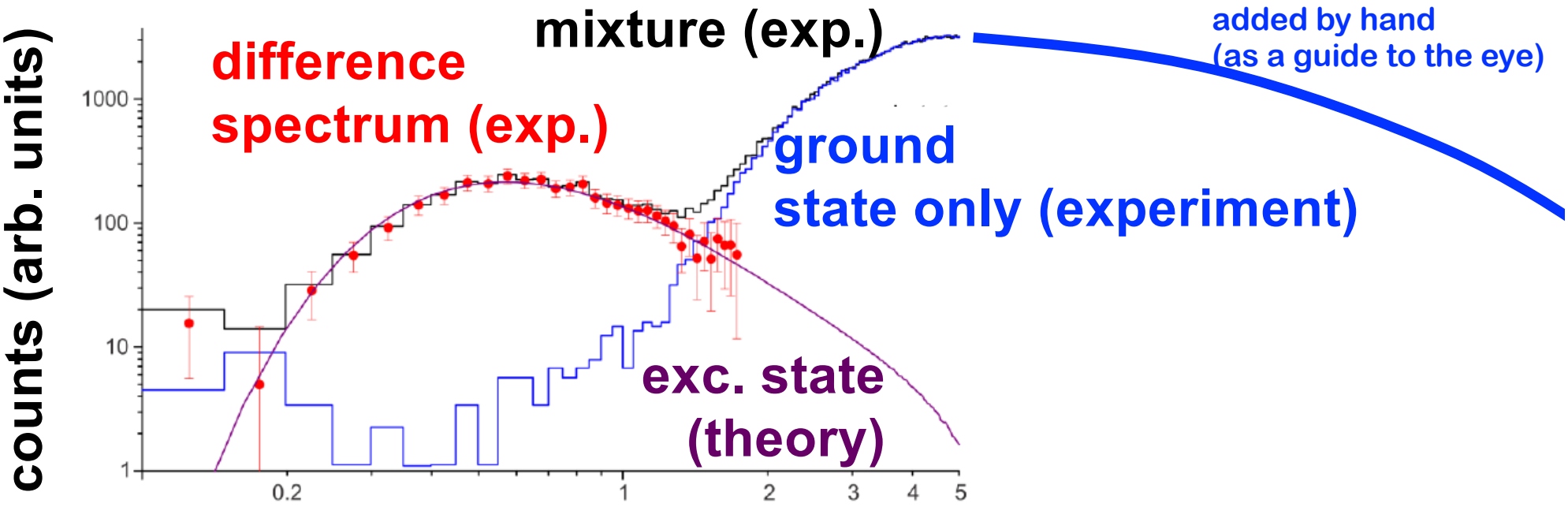

The ionization is instantaneous and the He-ions are distributed according to the quantum mechanical eigen states of the ground and excited helium trimers.

Large r_{12}, r_{23} and r_{31} correspond to small KER=$1/r_{12}+1/r_{23}+1/r_{31}$.

Reconstructing Real Space Properties

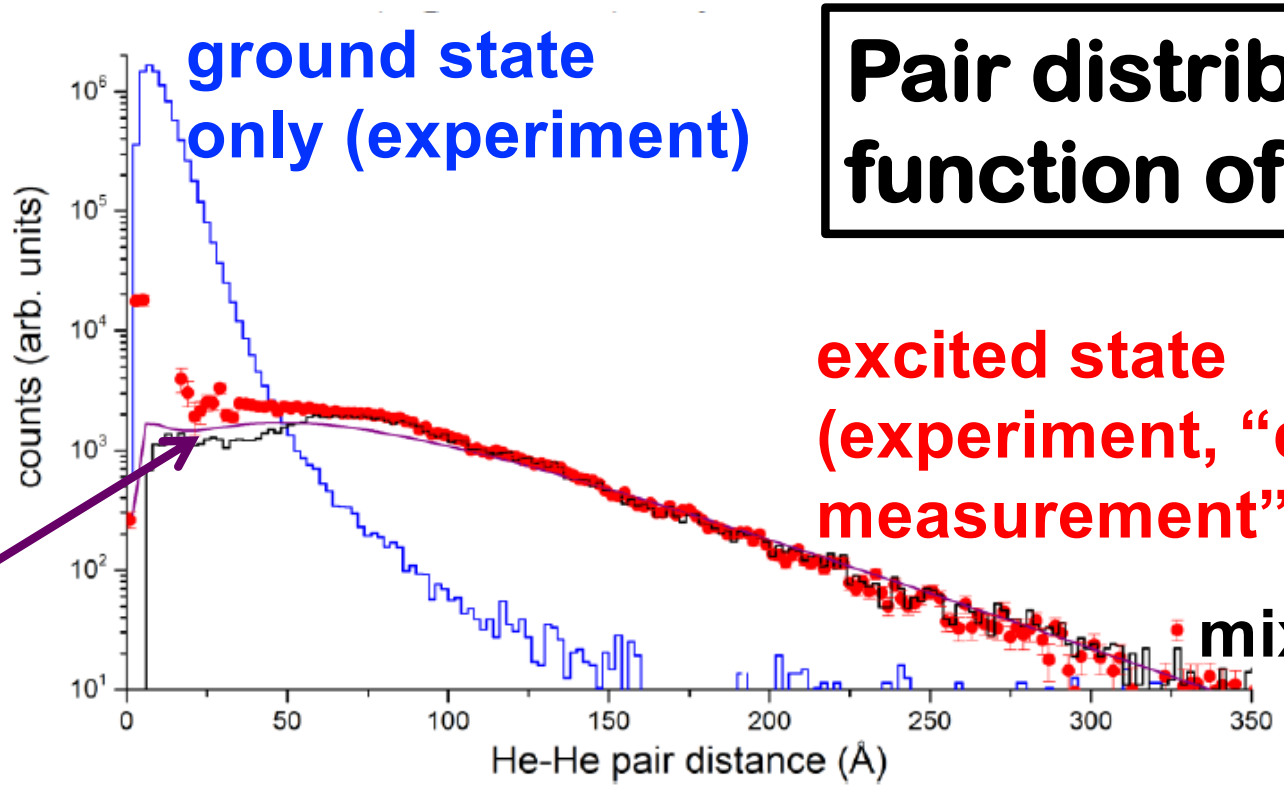

Pair distribution function of $(^4He_3)^*$

excited state (experiment, "difference measurement")

mixture (exp.)

excited state (theory)

The excited state is eight times larger than the ground state.
Assuming an "atom-dimer geometry", the tail can be fit to extract the binding energy of the excited helium trimer.
Fit to experimental data yields 2.6(2)mK.
Theory 2.65mK [Hiyama et al., PRA 85, 062505 (2012)].

Normalized Structural Properties of $^4He_3$

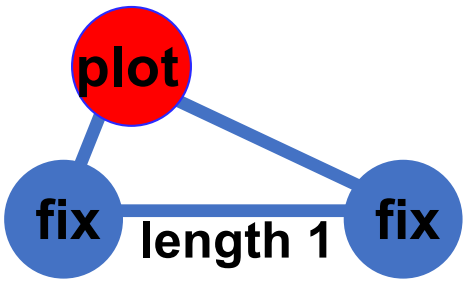

excited state: theory

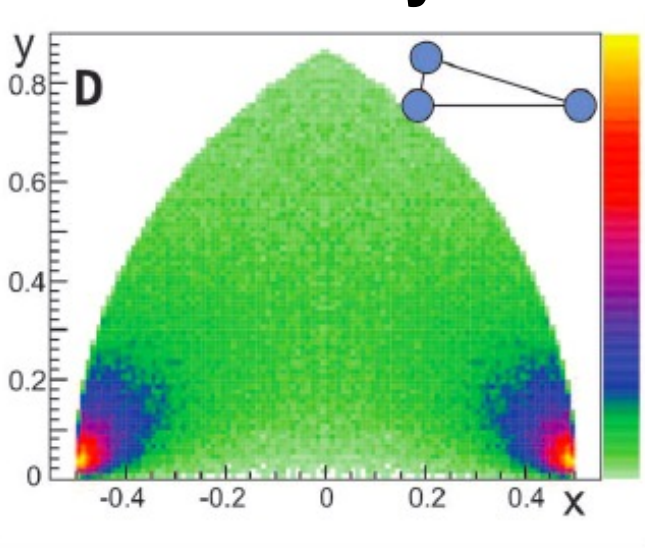

excited state: experiment

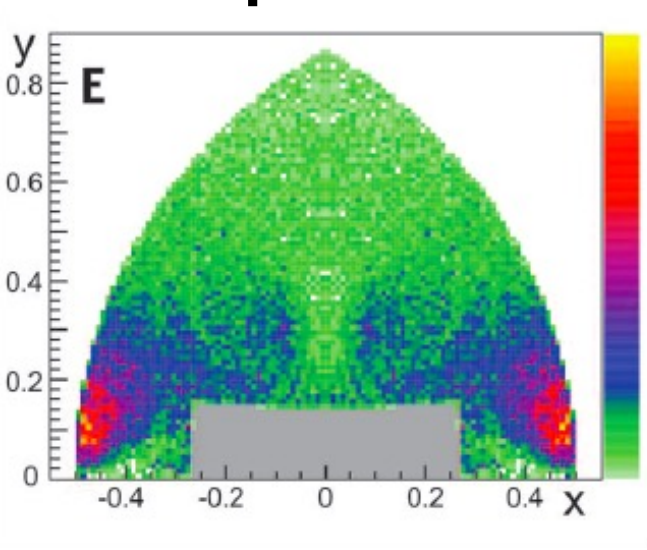

ground state: theory

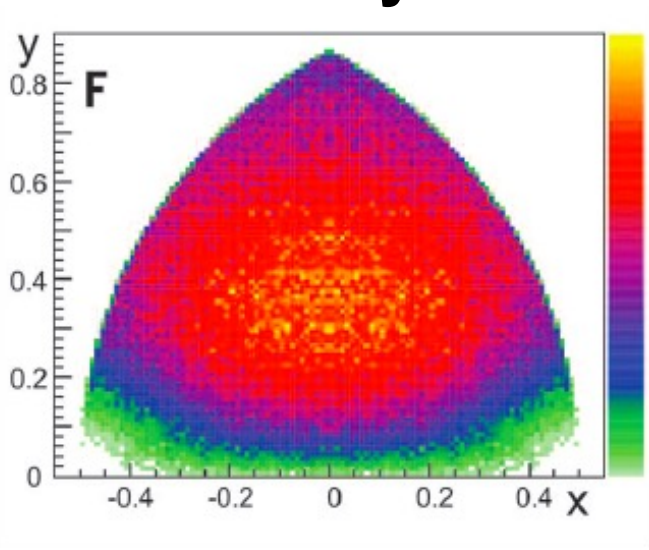

Divide all three interparticle distances by largest r_{ij} and plot k^{th} atom (positive y): Corresponds to placing atoms i and j at (−1/2,0) and (1/2,0).

Ground state and excited states have distinct characteristics!!!

Message: Reconstruction of quantum mechanical trimer density.

Summary of Introductory Part

- ^4He_N droplets can be realized experimentally in size-selective manner.
- Access to structural properties (accessing real-space structures beyond N=3 is non-trivial due to reconstruction algorithm).
- ^4He-^4He well described by effective range theory (two-parameter theory).
- $^4He_3$: Ground state has Efimov characteristics and excited state is Efimov trimer (s-wave scattering length and three-body parameter).

- If we want more "info," what can be done?
  - Spectroscopy (need more than one bound energy level).
  - Isotope substitution ($^4He \rightarrow {}^3He$).
  - Tuning of interactions (this talk: ground state droplets).
  - Dynamics (this talk: dimer).

Structural Properties: Short- and Long-Range Characteristics

Emphasized during introductory part:

- Universal long-range behavior ($r \gg r_{eff}$).
- Large probability to find particles at large separations.
- Low-energy theory starts with s-wave scattering length and then systematically adds corrections.

Atomic systems:

- Van der Waals universality.
- Highly repulsive short-range potential.

Which long-range behaviors "collapse"?
Which short-range behaviors "collapse"?

Strategy: Consider different two-body potentials (realistic and effective models), both at the physical point and at unitarity.

Different (Helium-Helium) Interaction Potentials

Strategy: Consider different two-body potentials [realistic (Model I) and effective models (Model II)], both at the physical point and at unitarity.

Model I: Realistic potential with hard inner wall.

$$V_{tot} = \sum_{j=1}^{N-1} \sum_{k>j}^{N} V_{realistic}(r_{jk})$$

Unitarity realized by applying overall scaling factor.

HFD-HE2.
CPKMJS.
TTY.
LM2M2.

Model II: Effective low-energy potential model.

$$V_{tot} = \sum_{j=1}^{N-1} \sum_{k>j}^{N} V_{2,gauss}(r_{jk}) + \sum_{j=1}^{N-2} \sum_{k>j}^{N-1} \sum_{l>k}^{N} V_{3,gauss}(R_{jkl})$$

matched to HFD-HE2 and scaled-HFD-HE2.

See Kievsky et al., PRA 96, 040501 (2017); PRA 102, 063320 (2020):
2-body range and depth → s-wave scattering length and effective range.
3-body range and depth → three- and four-body energy.

Diffusion Monte Carlo: Unbiased Energies

dimer (physical point)

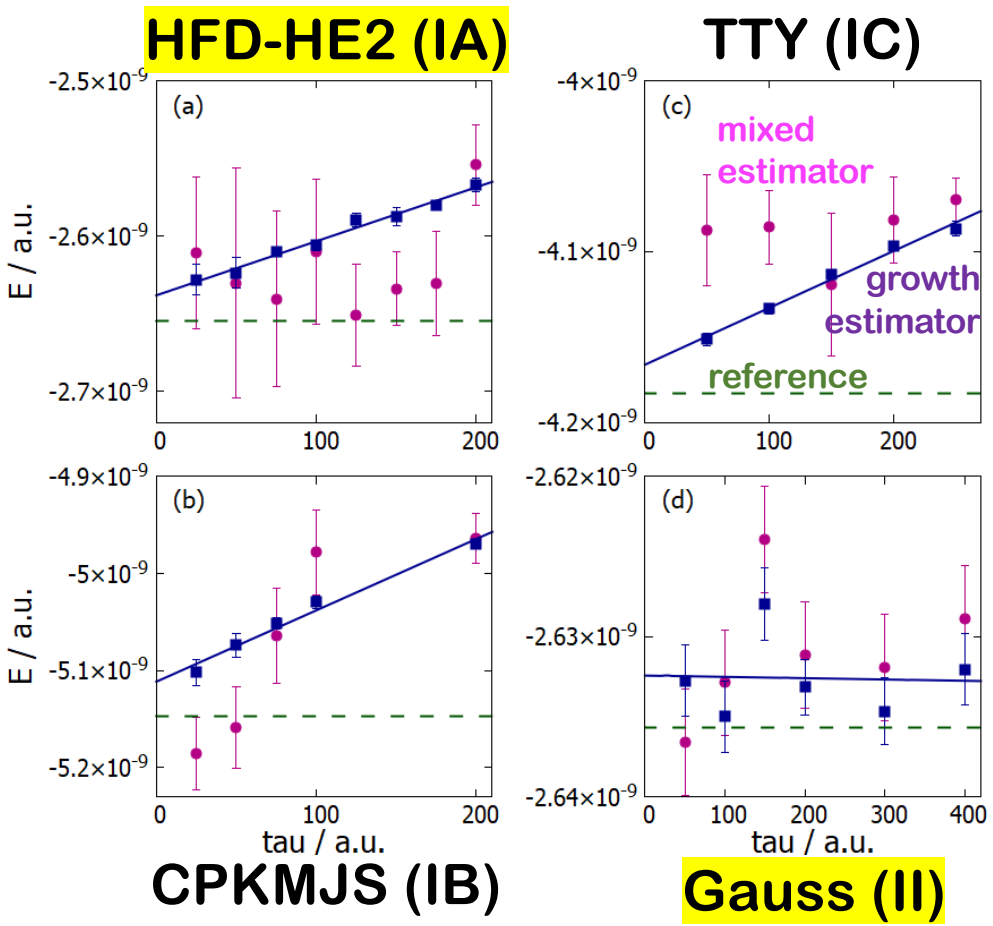

trimer (phys. & unit.)

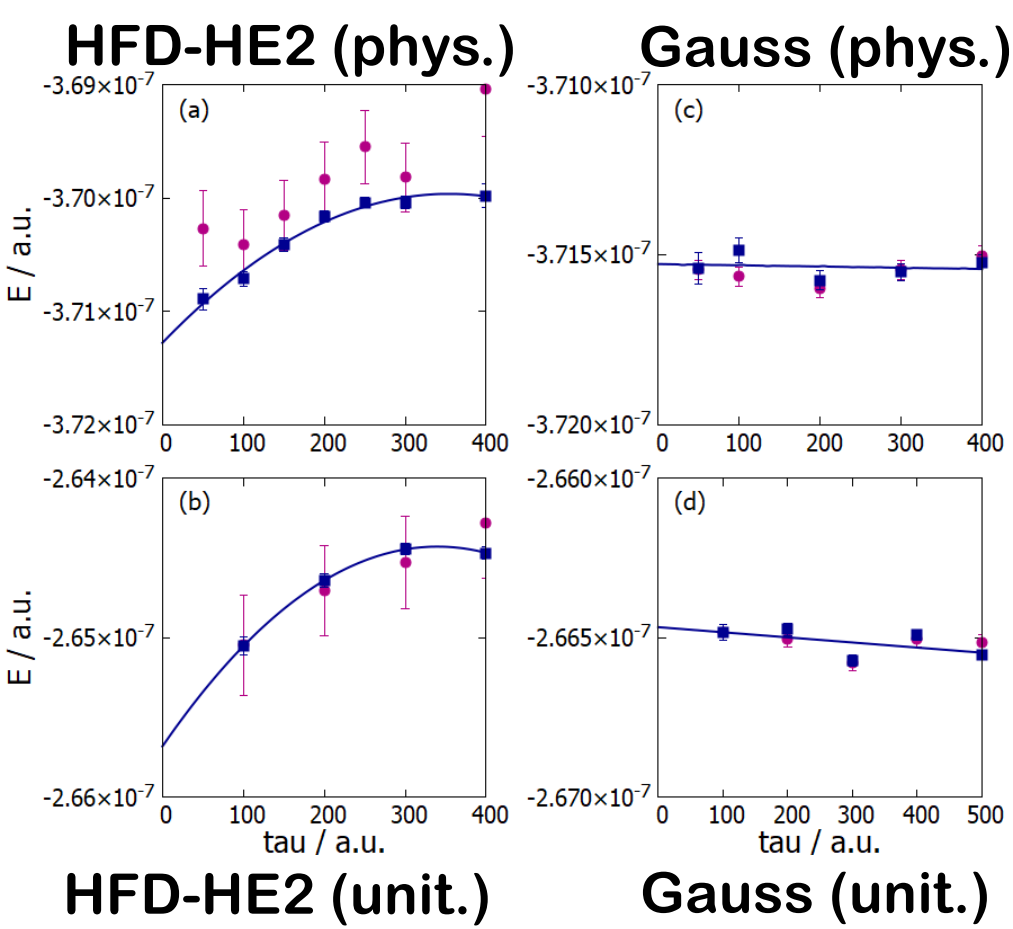

Diffusion Monte Carlo: Unbiased Energies

Physical point:

N	$E_{\text{HFD-HE2}}{}^{(d)}$ (Model IA)	E_{CPKMJS} (Model IB)	E_{TTY} (Model IC)	E_{GAUSS} (Model II)	$E_{\text{CPKMJS}}/E_{\text{HFD-HE2}}$ (in percent)	$E_{\text{GAUSS}}/E_{\text{HFD-HE2}}$ (in percent)
$2^{(a)}$	-2.645×10^{-9}	-5.147×10^{-9}	-4.183×10^{-9}	-2.6357×10^{-9}	195	100
$3^{(b)}$	$-3.713(3) \times 10^{-7}$	$-4.174(5) \times 10^{-7}$	$-4.006(3) \times 10^{-7}$	$-3.715(1) \times 10^{-7}$	112	100
$4^{(c)}$	$-1.688(1) \times 10^{-6}$	$-1.815(1) \times 10^{-6}$	$-1.768(1) \times 10^{-6}$	$-1.6984(1) \times 10^{-6}$	108	101
$5^{(c)}$	$-3.966(1) \times 10^{-6}$	$-4.201(1) \times 10^{-6}$	$-4.112(1) \times 10^{-6}$	$-3.9622(3) \times 10^{-6}$	106	100
$6^{(c)}$	$-7.102(2) \times 10^{-6}$	$-7.467(2) \times 10^{-6}$	$-7.325(1) \times 10^{-6}$	$-7.0166(4) \times 10^{-6}$	105	99
$7^{(c)}$	$-1.0986(5) \times 10^{-5}$	$-1.150(1) \times 10^{-5}$	$-1.130(1) \times 10^{-5}$	$-1.0737(1) \times 10^{-5}$	106	98
$8^{(c)}$	$-1.5531(6) \times 10^{-5}$	$-1.621(1) \times 10^{-5}$	$-1.594(1) \times 10^{-5}$	$-1.5030(1) \times 10^{-5}$	104	97
$9^{(c)}$	$-2.066(1) \times 10^{-5}$	$-2.152(1) \times 10^{-5}$	$-2.1176(8) \times 10^{-5}$	$-1.9830(2) \times 10^{-5}$	104	96
$10^{(c)}$	$-2.631(1) \times 10^{-5}$	$-2.736(1) \times 10^{-5}$	$-2.694(1) \times 10^{-5}$	$-2.5083(2) \times 10^{-5}$	104	95

Unitarity:

N	$E_{\text{HFD-HE2}}{}^{(d)}$ (Model IA)	E_{CPKMJS} (Model IB)	E_{GAUSS} (Model II)	$E_{\text{CPKMJS}}/E_{\text{HFD-HE2}}$ (in percent)	$E_{\text{GAUSS}}/E_{\text{HFD-HE2}}$ (in percent)
$3^{(b)}$	$-2.656(6) \times 10^{-7}$	$-2.65(1) \times 10^{-7}$	$-2.665(1) \times 10^{-7}$	100	100
$4^{(c)}$	$-1.391(1) \times 10^{-6}$	$-1.395(5) \times 10^{-6}$	$-1.4028(1) \times 10^{-6}$	100	101
$5^{(c)}$	$-3.411(3) \times 10^{-6}$	$-3.418(4) \times 10^{-6}$	$-3.4130(2) \times 10^{-6}$	100	100
$6^{(c)}$	$-6.235(6) \times 10^{-6}$	$-6.241(4) \times 10^{-6}$	$-6.1642(4) \times 10^{-6}$	100	99
$7^{(c)}$	$-9.764(9) \times 10^{-6}$	$-9.773(4) \times 10^{-6}$	$-9.5379(6) \times 10^{-6}$	100	98
$8^{(c)}$	$-1.391(1) \times 10^{-5}$	$-1.392(8) \times 10^{-5}$	$-1.3446(1) \times 10^{-5}$	100	97
$9^{(c)}$	$-1.861(1) \times 10^{-5}$	$-1.863(10) \times 10^{-5}$	$-1.7824(1) \times 10^{-5}$	100	96
$10^{(c)}$	$-2.379(2) \times 10^{-5}$	$-2.382(12) \times 10^{-5}$	$-2.2626(2) \times 10^{-5}$	100	95

^4He_N: N^{th} Atom Relative to Center-of-Mass of N-1 Atoms

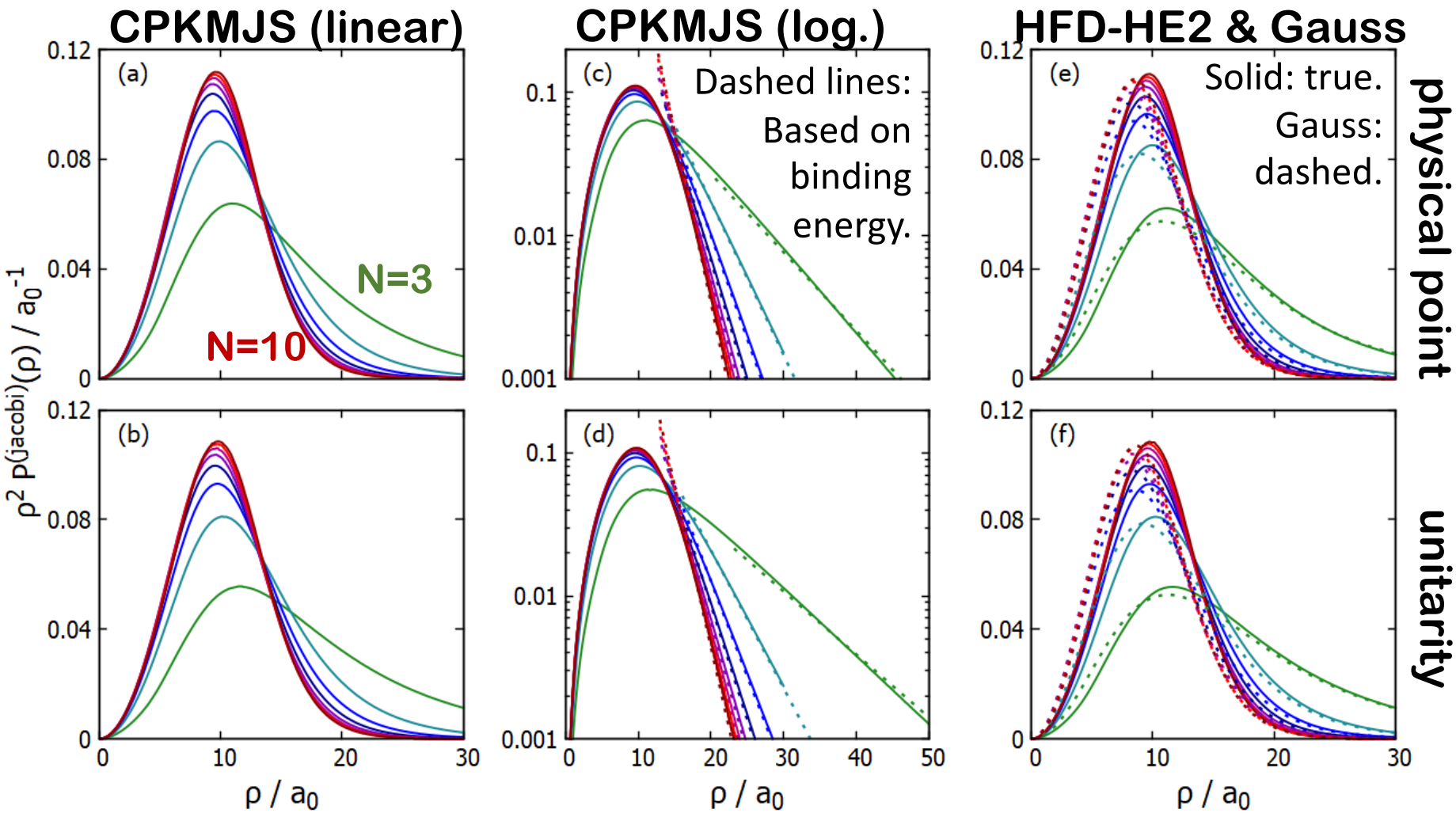

Results obtained using forward walking: Reynolds et al., J. Stat. Phys. 43, 1017 (1986).

Pair Distribution Function $P^{(2)}(r)$ for $N = 2 - 10$

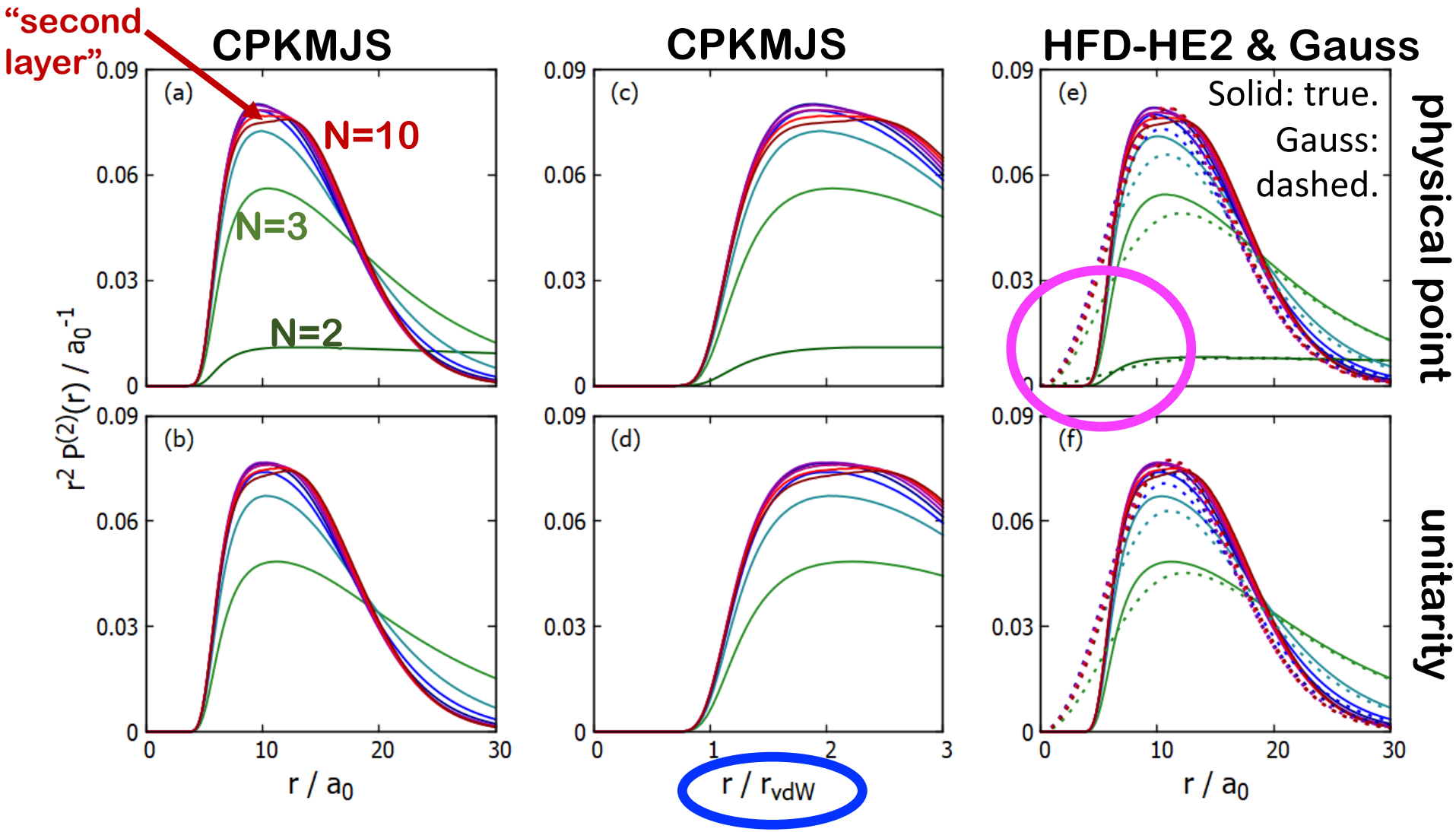

Contrasting with Two-Component Fermions at Unitarity

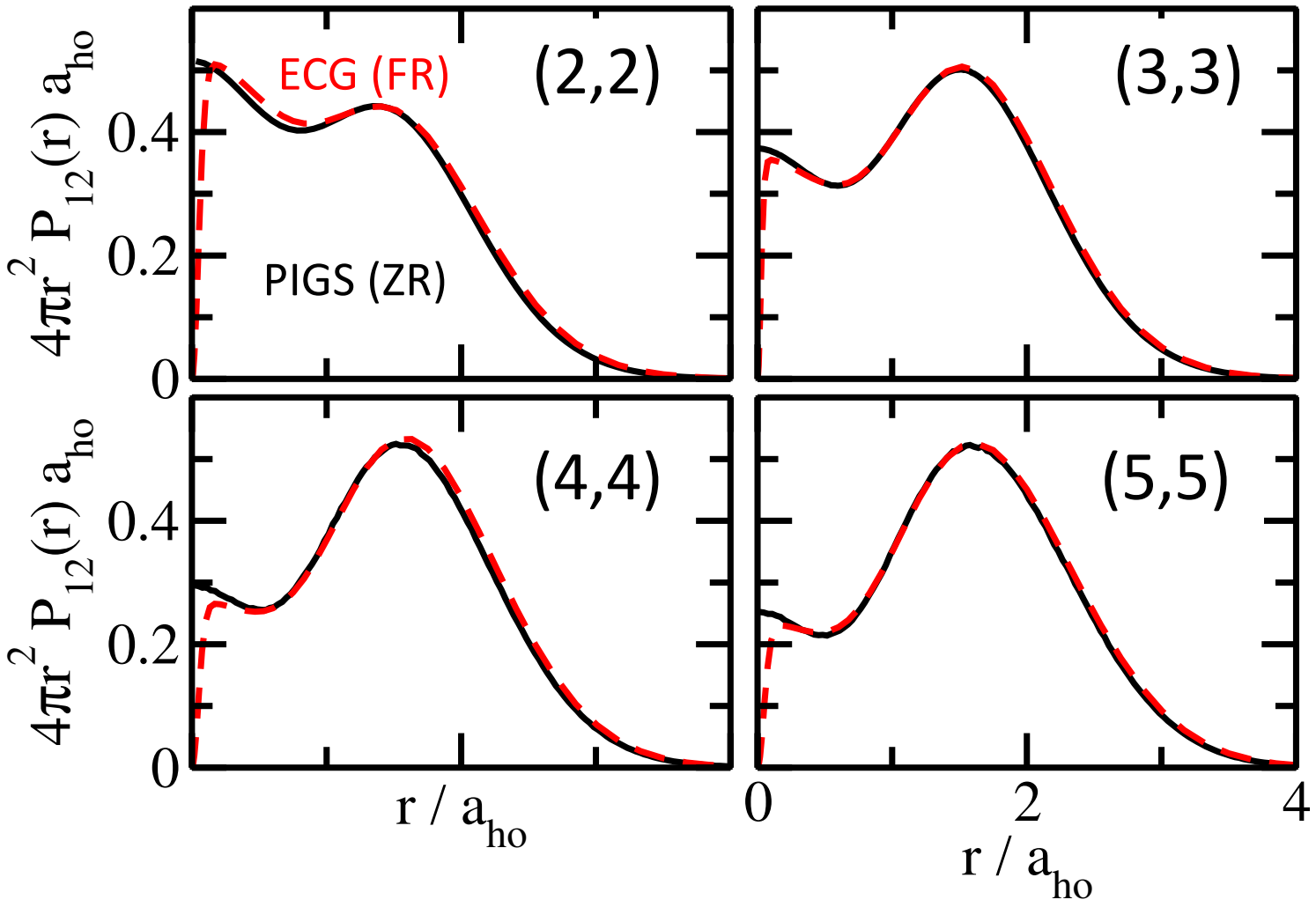

$(N_\uparrow, N_\downarrow)$ system with infinitely large s-wave scattering length under spherically symmetric harmonic confinement (ground state).

$P^{(2)}(r)$, Two-Body Contact $C_N^{(2)}$, van der Waals Universality

$$\hat{P}_N^{(2)}(r) = \frac{2}{N(N-1)} \sum_{j=1}^{N-1} \sum_{k>j}^{N} \frac{\delta(r_{j,k} - r)}{r^2}$$

$$\int_0^\infty P_N^{(2)}(r) r^2 dr = 1$$

$$P_N^{(2)}(r) \underset{\text{small } r}{\rightarrow} C_N^{(2)} P_2^{(2)}(r)$$

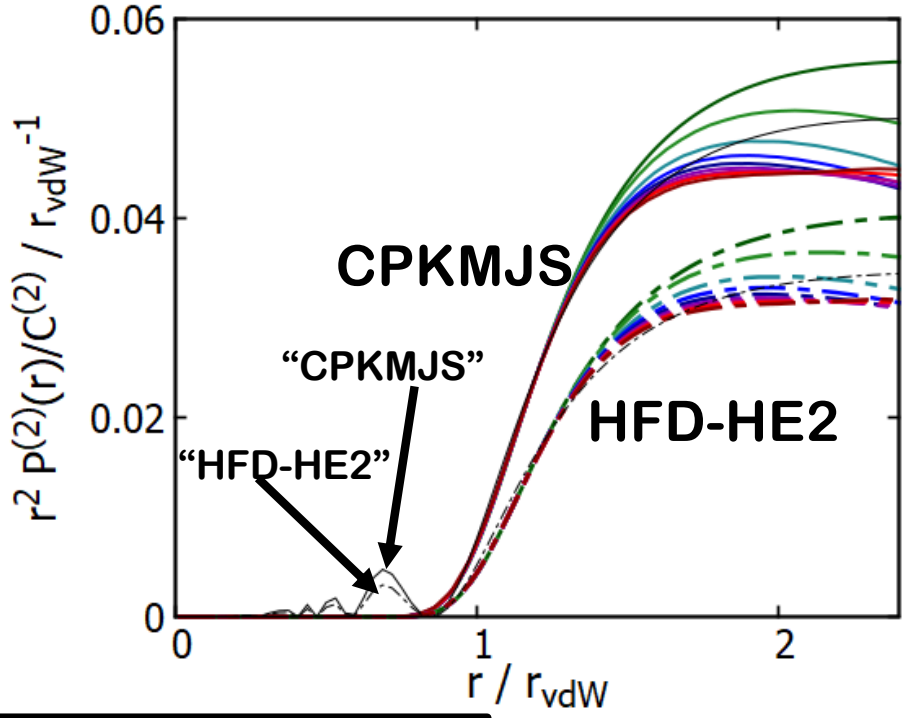

$\frac{a_s}{r_{vdW}} = 46.95$ for HFD-HE2.

$\frac{a_s}{r_{vdW}} = 33.63$ for CPKMJS.

See Naidon et al., PRL 112, 105301 (2014); PRA 90, 022106 (2014) for vdW universality of trimer at unitarity.

$$\varphi_{\text{vdW}}(r) = B\left[\Gamma(5/4)x^{1/2}J_{1/4}(2x^{-2}) - \frac{r_{\text{vdW}}}{a_s}\Gamma(3/4)x^{1/2}J_{-1/4}(2x^{-2})\right]$$

Flambaum et al., PRA 59, 1998 (1999).
Gao, PRA 58, 4222 (1998).

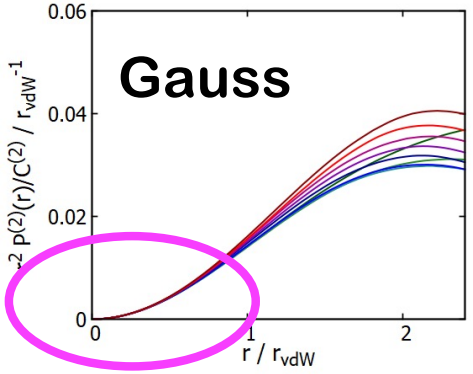

$P^{(2)}(r)$, Two-Body Contact $C_N^{(2)}$, van der Waals Universality

$$\hat{P}_N^{(2)}(r) = \frac{2}{N(N-1)} \sum_{j=1}^{N-1} \sum_{k>j}^{N} \frac{\delta(r_{j,k} - r)}{r^2}$$

$$\int_0^\infty P_N^{(2)}(r) r^2 dr = 1$$

$$P_N^{(2)}(r) \underset{\text{small } r}{\rightarrow} C_N^{(2)} P_2^{(2)}(r)$$

N	$C_N^{(2)}N(N-1)/2$ HFD-HE2	$C_N^{(2)}N(N-1)/2$ CPKMJS	$C_N^{(2)}N(N-1)/2$ TTY	$C_N^{(2)}N(N-1)/2$ LM2M2 [34]	HFD-HE2/CPKMJS (in percent)	TTY/CPKMJS (in percent)	LM2M2/CPKMJS (in percent)
2	1	1	1	1	100	100	100
3	22.3	16.9	18.4	17.8(0.03)	132	109	106
4	62.4	46.2	50.5	48.8(1)	135	109	106
5	117	86.1	94.2	91.1(3)	136	109	106
6	184	134	147	143(0.6)	137	110	106
7	259	189	207	201(0.8)	137	110	106
8	343	250	274	267(1)	138	110	107
9	434	315	346	338(2)	138	110	107
10	533	386	424	415(2)	138	110	108

Assuming that the pair distribution functions for different potential models agree for larger N, we find that the ratio of the two-body contacts for larger N is given, to leading order, by the ratio between a_s/r_{vdW} for the two interaction potentials.

1.40 **1.10** **1.13**

Bazak et al., PRA 101, 010501 (2020)

Yates, Blume, PRA 105, 022824 (2022)

See Kim et al., Annu. Rev. Nucl. Sci. 24, 96 (1974): "asymptotic normalization constant"

Three-Body (Sub-Cluster) Correlations for $N = 3 - 10$

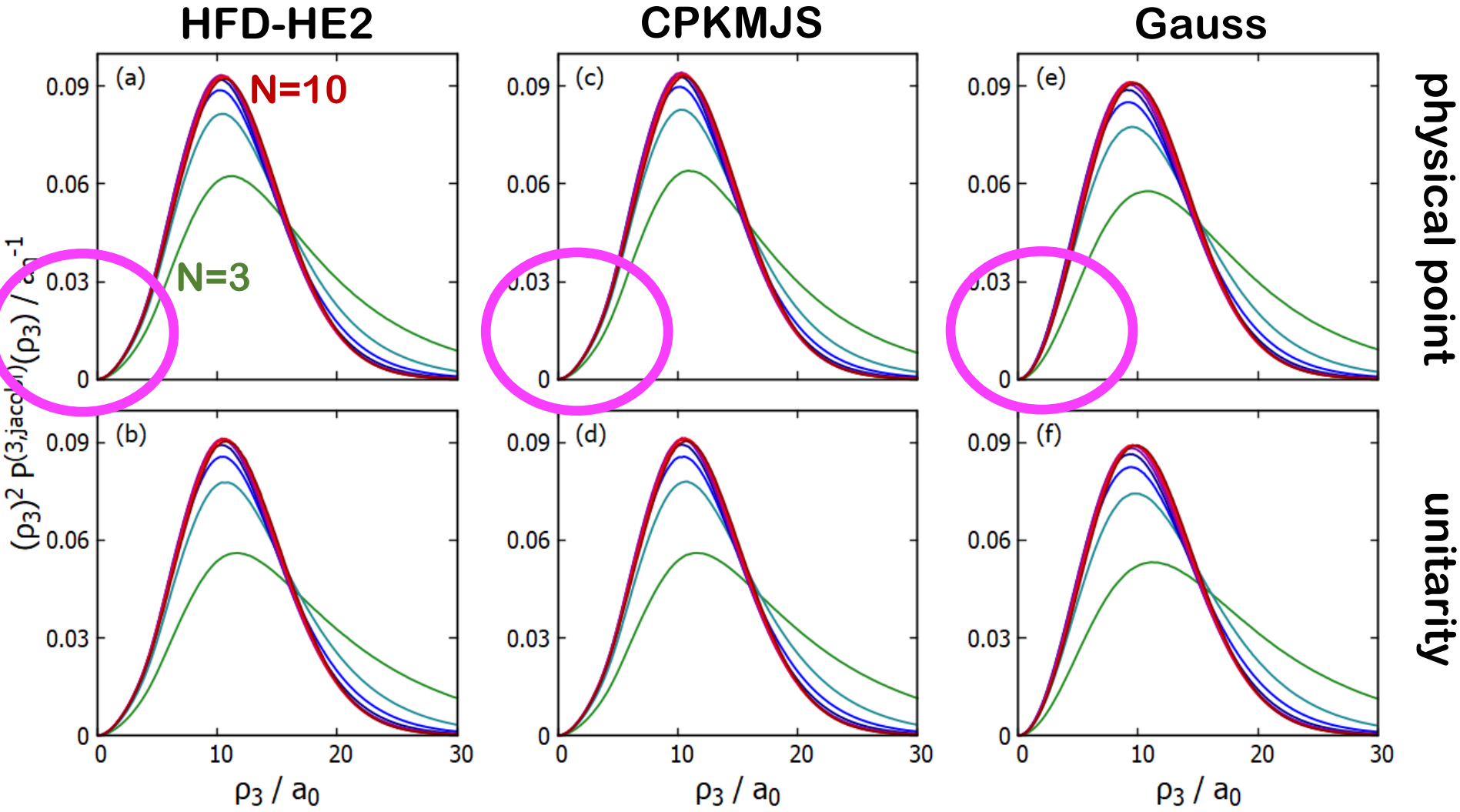

Short-Range “2+1 Contact”

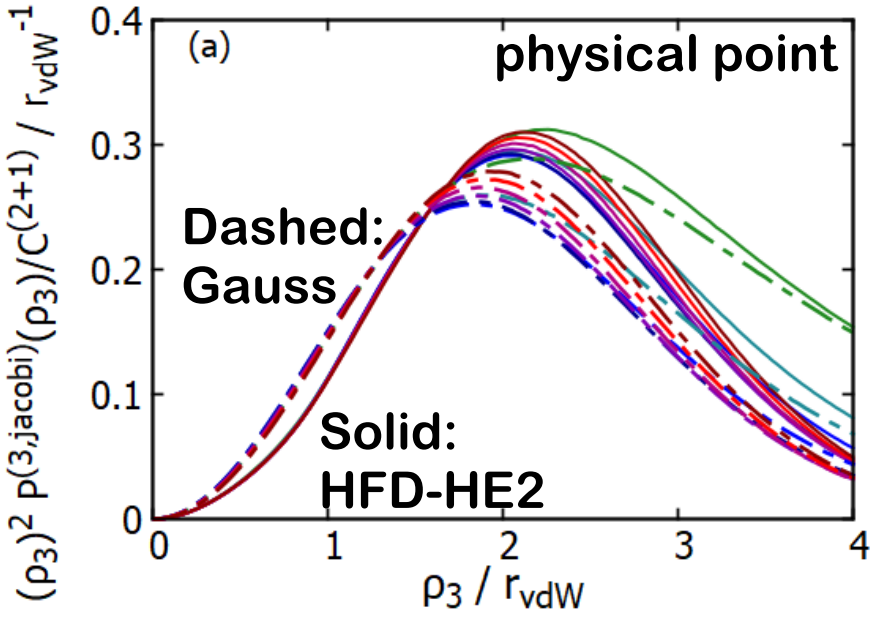

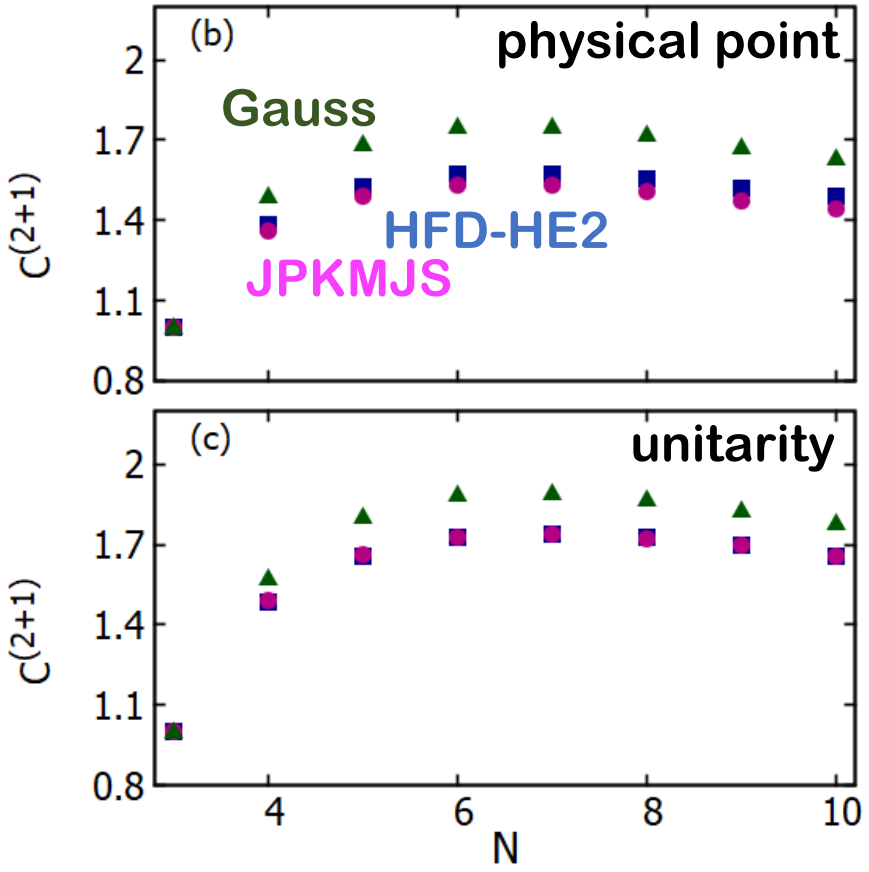

$$P_N^{(3,\mathrm{jacobi})}(\rho_3) \underset{\text{small } \rho_3}{\rightarrow} C_N^{(2+1)} P_3^{(3,\mathrm{jacobi})}(\rho_3)$$

$$\Psi(\vec{r}_1, \cdots, \vec{r}_N) \underset{\text{small } \rho_{jk,l}}{\rightarrow} \Phi(\vec{\rho}_{jk,l}) B_N^{(2+1)}(\vec{r}_{j,k}, \vec{R}_{j,k,l}, \{\vec{r}_{n;n\neq j,k,l}\})$$

Summary

- ^4He_N droplets can be realized experimentally in size-selective manner.
- Access to structural properties (accessing real-space structures beyond N=3 is non-trivial due to reconstruction algorithm).
- ^4He-^4He well described by effective range theory (two-parameter theory).
- $^4He_3$: Ground state has Efimov characteristics and excited state is Efimov trimer (s-wave scattering length and three-body parameter).

- If we want more "info," what can be done?
  - Spectroscopy (need more than one bound energy level).
  - Isotope substitution ($^4He \rightarrow {}^3He$).
  - Tuning of interactions (this talk: ground state droplets).
  - Dynamics (this talk: dimer).

Basic Concept

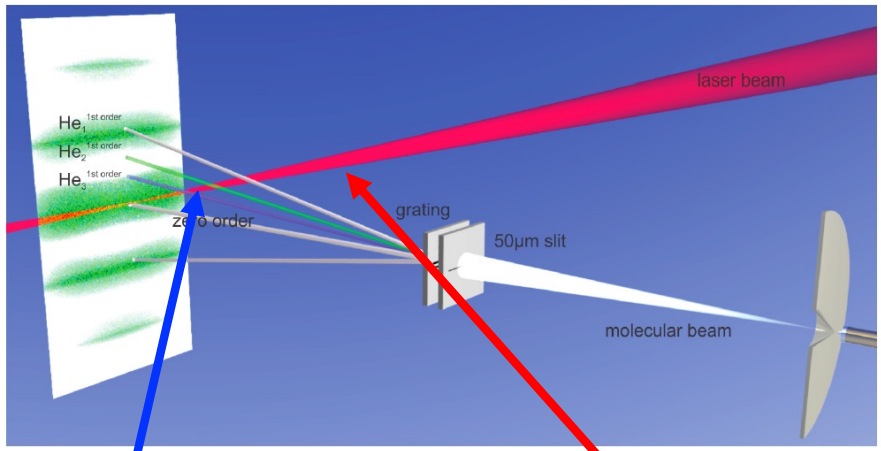

Prepare universal initial state (i.e., state that is dominated by s-wave scattering length).

Interrogate the initial state: fast and intense pump laser that takes the system out of equilibrium.

Wait for a variable time (delay) and apply even shorter and more intense probe laser that allows us to look at time-evolved system.

Basic Concept

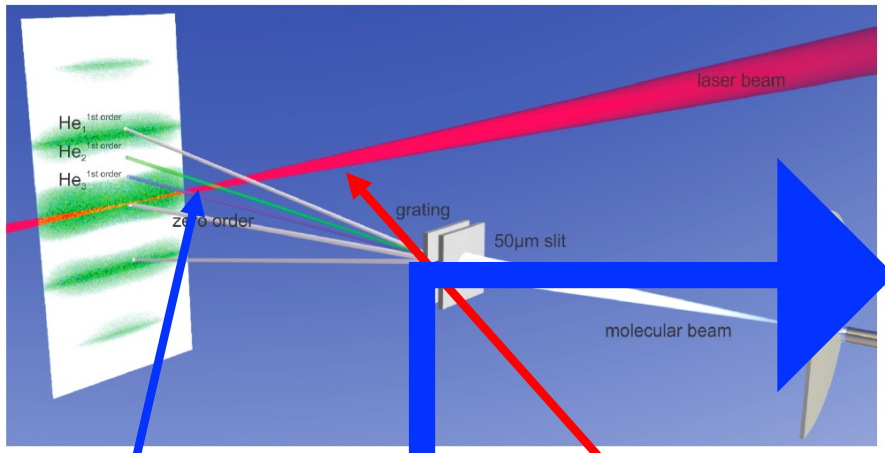

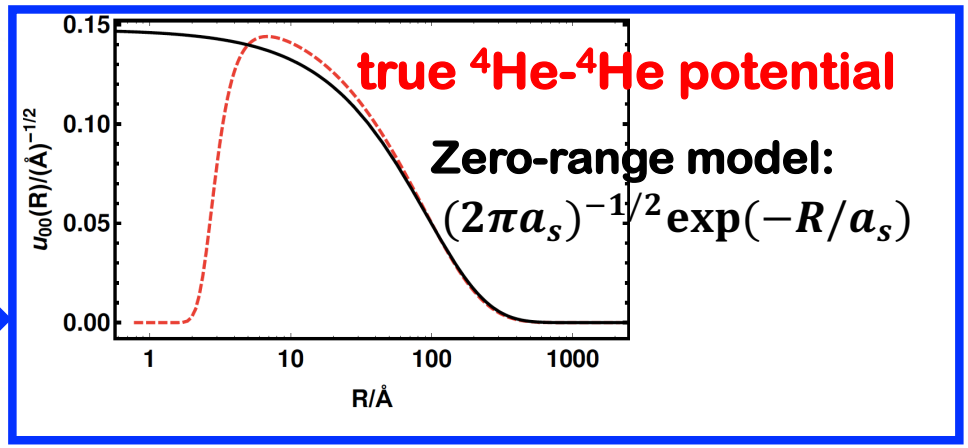

Prepare universal initial state (i.e., state that is dominated by s-wave scattering length).

Interrogate the initial state: fast and intense pump laser that takes the system out of equilibrium.

Wait for a variable time (delay) and apply even shorter and more intense probe laser that allows us to look at time-evolved system.

Basic Concept

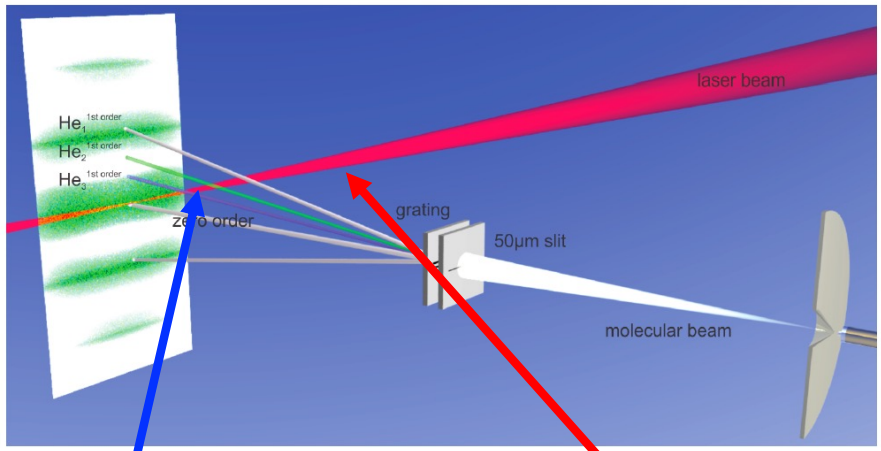

Sort of like…

From vectorstock.com

Prepare universal initial state (i.e., state that is dominated by s-wave scattering length).

Interrogate the initial state: fast and intense pump laser that takes the system out of equilibrium.

Wait for a variable time (delay) and apply even shorter and more intense probe laser that allows us to look at time-evolved system.

Two Exciting Fields

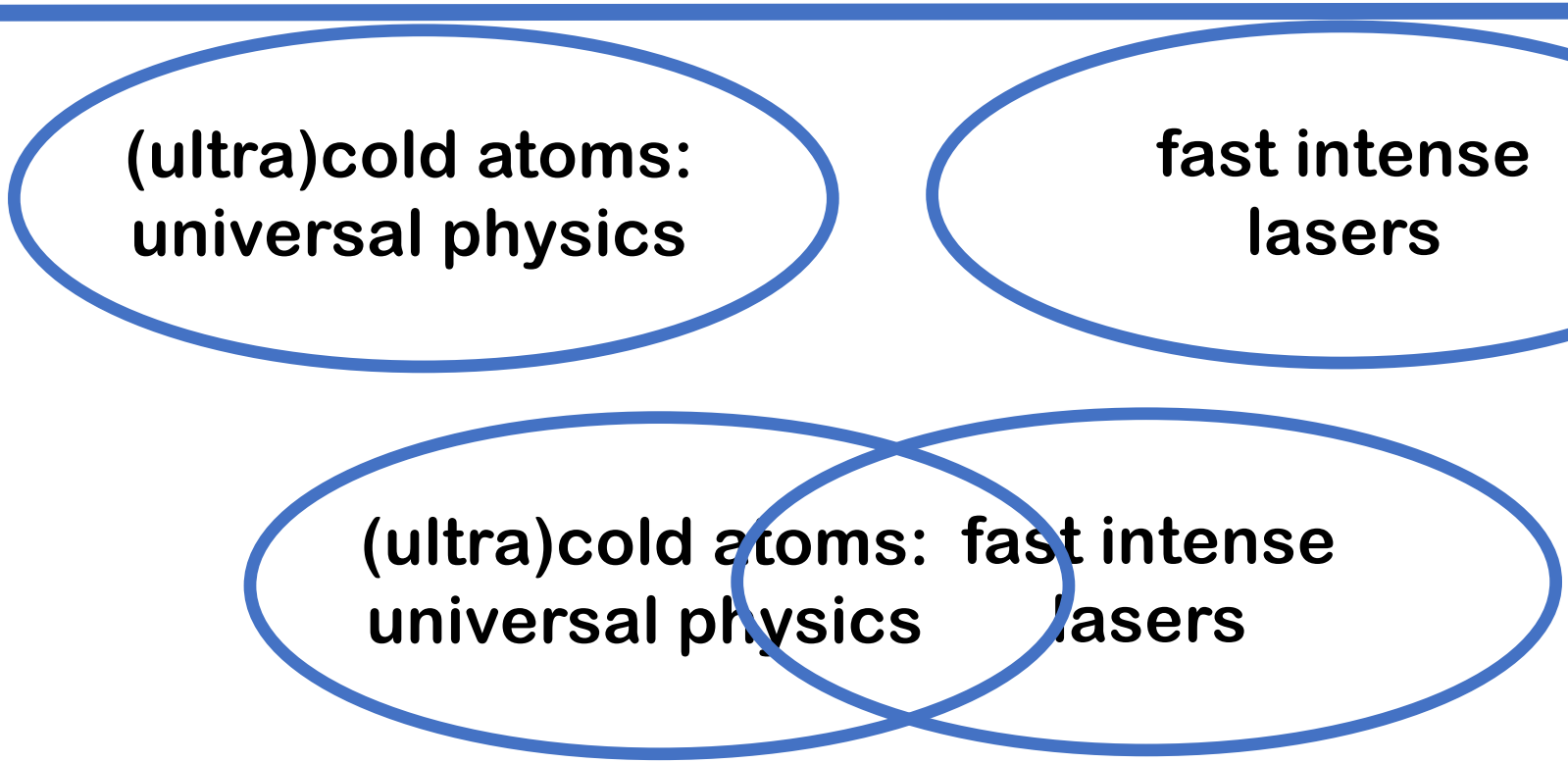

Selected Works in This Direction

PHYSICAL REVIEW LETTERS **124,** 253201 (2020)

ARTICLE

DOI: 10.1038/s41467-018-04556-3 OPEN

Quantum simulation of ultrafast
trapped ultracold atoms

Ruwan Senaratne[1], Shankari V. Rajagopal[1], Toshihiko Shimasaki[1], Peter E. Dotti[1], Kurt M. Fujiwara[1], Kevin [illegible][1]
Zachary A. Geiger[1] & David M. Weld[1]

Ultrafast Creation of Overlapping Rydberg Electrons in an Atomic BEC and Mott-Insulator Lattice

M. Mizoguchi,[1,2] Y. Zhang,[1,3] M. Kunimi,[1] A. Tanaka,[1] S. Takeda,[1,2,†] N. Takei,[1,2,‡] V. Bharti,[1] K. Koyasu,[1,2]
T. Kishimoto,[4] D. Jaksch,[5,6] A. Glaetzle,[5,6] M. Kiffner,[5,6] G. Masella,[7] G. Pupillo,[7]
M. Weidemüller,[8,9] and K. Ohmori[1,2,*]

(ultra)cold atoms: fast intense universal physics lasers

Found Phys (2014) 44:813–818
DOI 10.1007/s10701-014-9773-5

Optically Engineered Quantum States in Ultrafast and Ultracold Systems

Kenji Ohmori

PRL **103,** 260401 (2009) PHYSICAL REVIEW LETTERS week ending 31 DECEMBER 2009

RAPID COMMUNICATIONS

PHYSICAL REVIEW A **95,** 011403(R) (2017)

Ultracold-atom quantum simulator for attosecond science

Simon Sala, Johann Förster, and Alejandro Saenz
AG Moderne Optik, Institut für Physik, Humboldt-Universität zu Berlin, Newtonstraße 15, 12489 Berlin, Germany
(Received 23 November 2016; published 25 January 2017)

Pump-Probe Spectroscopy of Two-Body Correlations in Ultracold Gases

Christiane P. Koch[1,*] and Ronnie Kosloff[2]

Laser spectroscopic characterization of the nuclear clock isomer ^{229m}Th

Johannes Thielking[1], Maxim V. Okhapkin[1], Przemysław Głowacki[1,†],
David M. Meier[1], Lars von der Wense[2], Benedict Seiferle[2],
Christoph E. Düllmann[3,4,5], Peter G. Thirolf[2], Ekkehard Peik[1]

1 Physikalisch-Technische Bundesanstalt, 38116 Braunschweig, Germany.
2 Ludwig-Maximilians-Universität München, 85748 Garching, Germany.
3 GSI Helmholtzzentrum für Schwerionenforschung GmbH, 64291 Darmstadt, Germany.
4 Helmholtz-Institut Mainz, 55099 Mainz, G
5 Johannes Gutenberg-Universität, 5509

The isotope ^{229}Th is the only nucleus
energy range of a few electron volts,
valence shell of atoms, but about four

his

TERS **124,** 253201 (2020)

ing Rydberg Electrons in an

AR
DOI
Q
tra
Ruw
Zac

(ultra
unive

Found Phys (2014) 44:813–818
DOI 10.1007/s10701-014-9773-5

Optically Engineered Quantum States in Ultr
and Ultracold Systems

Kenji Ohmori

PRL **103,** 260401 (2009)

Pump-Pro

Laser Probing of Neutron-Rich Nuclei in Light Atoms

Z.-T. Lu

Physics Division, Argonne National Laboratory, Lemont, Illinois 60439, USA and
Department of Physics and Enrico Fermi Institute, University of Chicago, Chicago, Illinois 60637, USA

P. Mueller

Physics Division, Argonne National Laboratory, Lemont, Illinois 60439, USA

G. W. F. Drake

Department of Physics, University of Windsor, Windsor, Ontario N9B 3P4 Canada

W. Nörtershäuser

Institut für Kernphysik, Technische Universität Darmstadt, 64289 Darmstadt, Germany

Steven C. Pieper

Physics Division, Argonne National Laboratory, Argonne, Illinois 60439, USA

Z.-C. Yan

State Key Laboratory of Magnetic Resonance and Atomic and Molecular Physics, Wuhan Institute of Physics and Mathematics, and Center for Cold Atom Physics, Chinese Academy of Sciences, Wuhan 430071, China and
Department of Physics, University of New Brunswick, Fredericton, New Brunswick E3B 5A3 Canada

(Dated: June 5 2013)

The neutron-rich ^{6}He and ^{8}He isotopes exhibit an exotic nuclear structure that consists of a tightly bound ^{4}He-like core with additional neutrons orbiting at a relatively large distance, forming a halo. Recent experimental efforts have succeeded in laser trapping and cooling these short-lived, rare

Christiane P. Koch[1,*] and Ronnie Kosloff[2]

Pump-Probe Spectroscopy of Isolated Helium Dimers

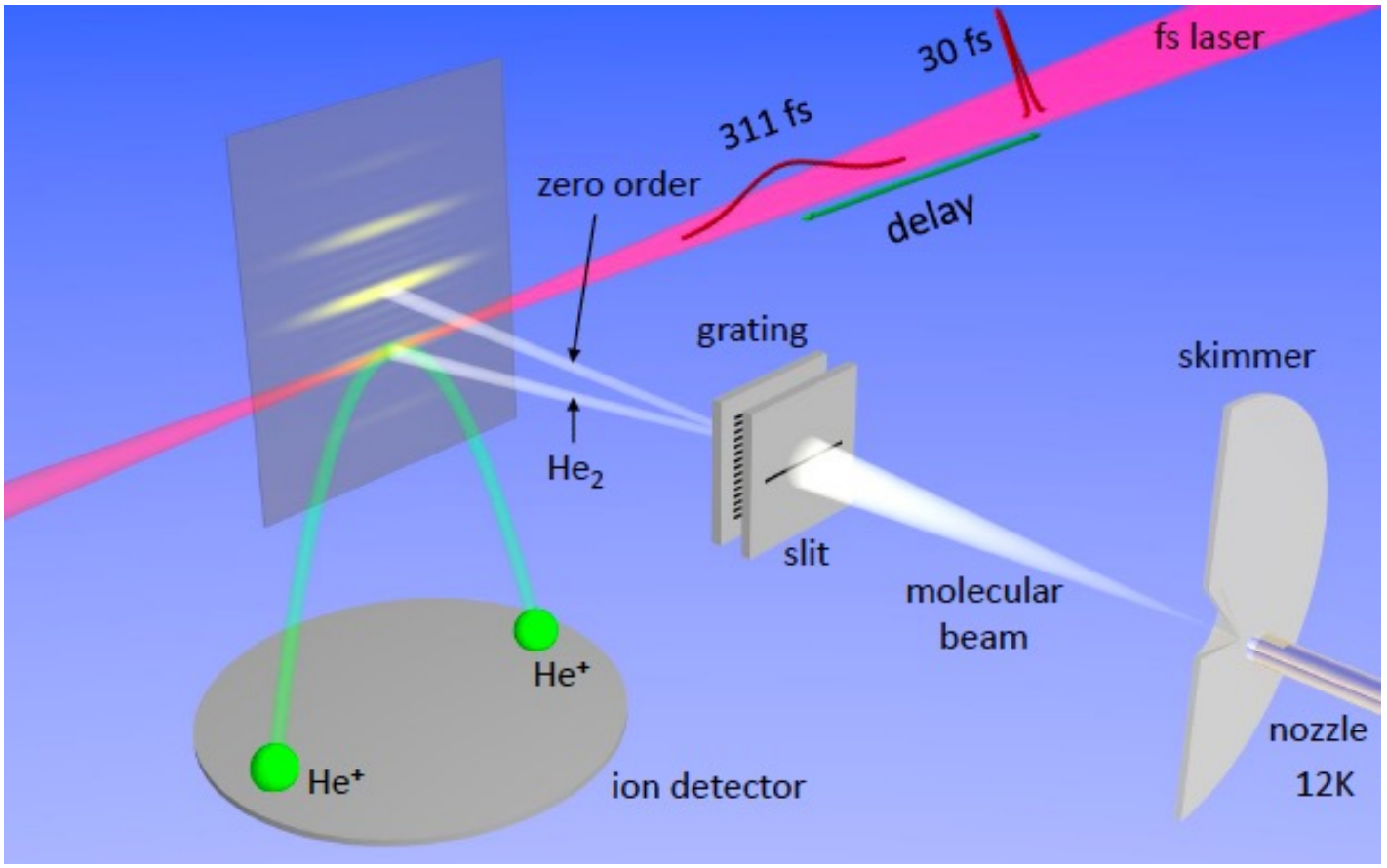

Pump pulse: pulse length of 311 fs and intensity of 1.3×10^{14} W/cm^2.
Probe pulse rips off two electrons (Coulomb explosion).
What do we expect to happen as a function of the delay time???

What Do The Numbers Mean?

Pump pulse: pulse length of 311 fs and intensity of 1.3×10^{14} W/cm^2.
Probe pulse: rips off two electrons (Coulomb explosion).
What do we expect to happen as a function of the delay time???

Binding energy of 1mK corresponds to $50\ \mathrm{ns} = 5 \cdot 10^7\ \mathrm{fs}$. The 311 fs pump laser is extremely short compared to the natural time scale of the helium dimer: laser pulse acts as a "kick."

Solar: $\frac{10^3 \mathrm{W}}{\mathrm{m}^2}$.

Laser pointer: $\frac{10^6 \mathrm{W}}{\mathrm{m}^2}$.

Pump pulse: $1.3 \cdot \frac{10^{13} W}{\mathrm{cm}^2} = 1.3 \cdot \frac{10^{17} \mathrm{W}}{\mathrm{m}^2}$.

Roughly, we need to worry about electronic degrees of freedom at intensities $> \frac{10^{15} \mathrm{W}}{\mathrm{cm}^2}$ (probe pulse).

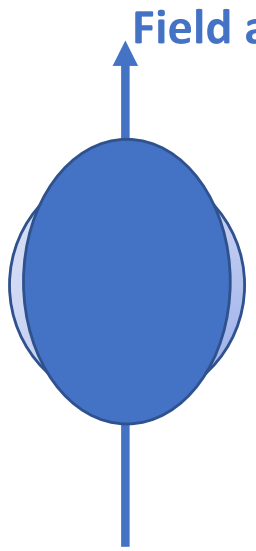

Laser pulse prepares new initial state (not an eigen state).

What Does The Pulse Do To Helium Dimer?

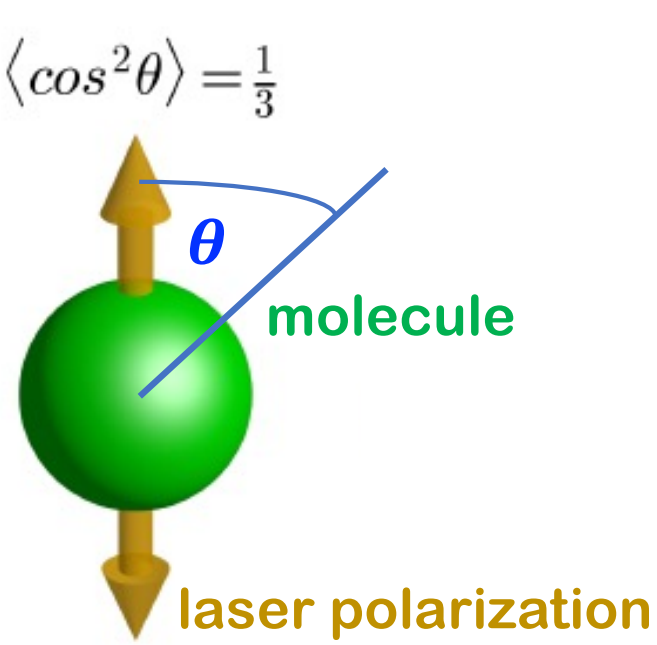

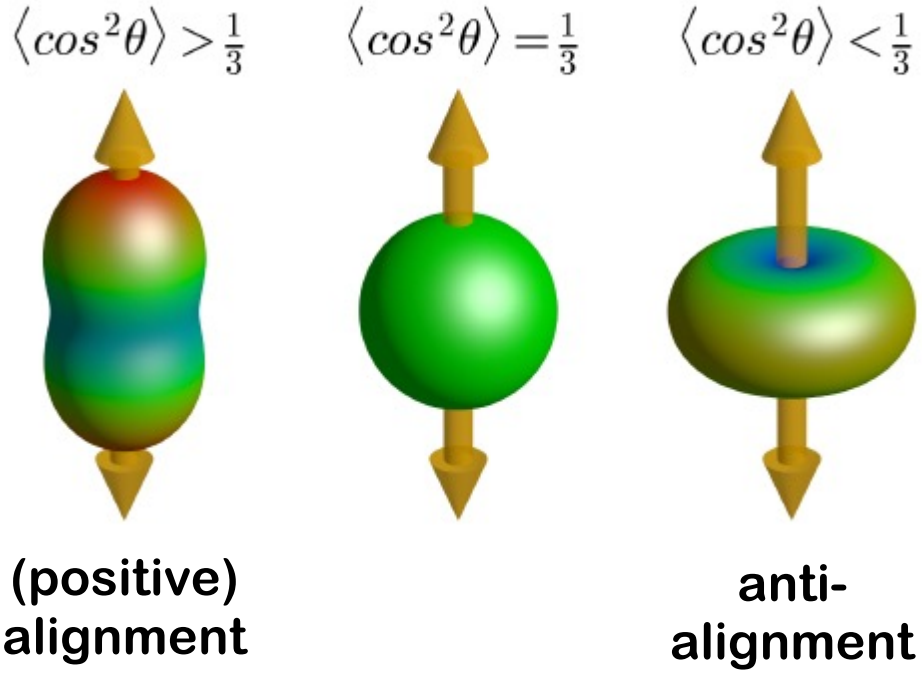

Without the laser, the molecule is spherically symmetric (no alignment): The helium dimer has vanishing relative orbital angular momentum.

Will show: Helium dimer can be aligned. However, since the $J > 0$ partial wave components are not bound, they will "run away" (dissociative wave packet). Heavier non-universal dimers behave very differently.

Pump-Probe Experiments: Field Induced Alignment

Long history of electric-field induced alignment of molecules: Unique rotational dynamics for molecules such as I_2, N_2,…

E.g., "Colloquium: Aligning molecules with strong laser pulses", RMP 75, 543 (2003) by Stapelfeldt and Seideman, >1000 citations:

"We review the theoretical and experimental status of intense laser alignment—a field at the interface between intense laser physics and chemical dynamics with potential applications ranging from high harmonic generation and nanoscale processing to stereodynamics and control of chemical reactions."

Work on helium dimer adds "physical dynamics" to the list!

Alignment $\langle cos^2\theta \rangle$ for N_2

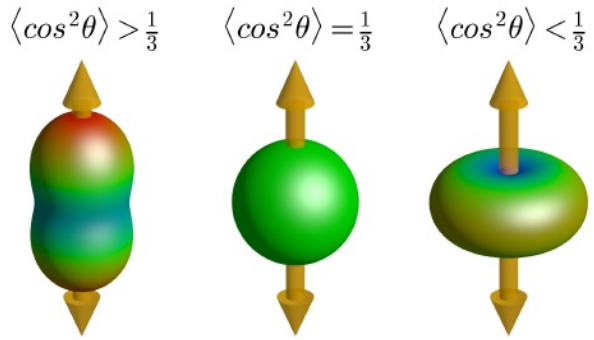

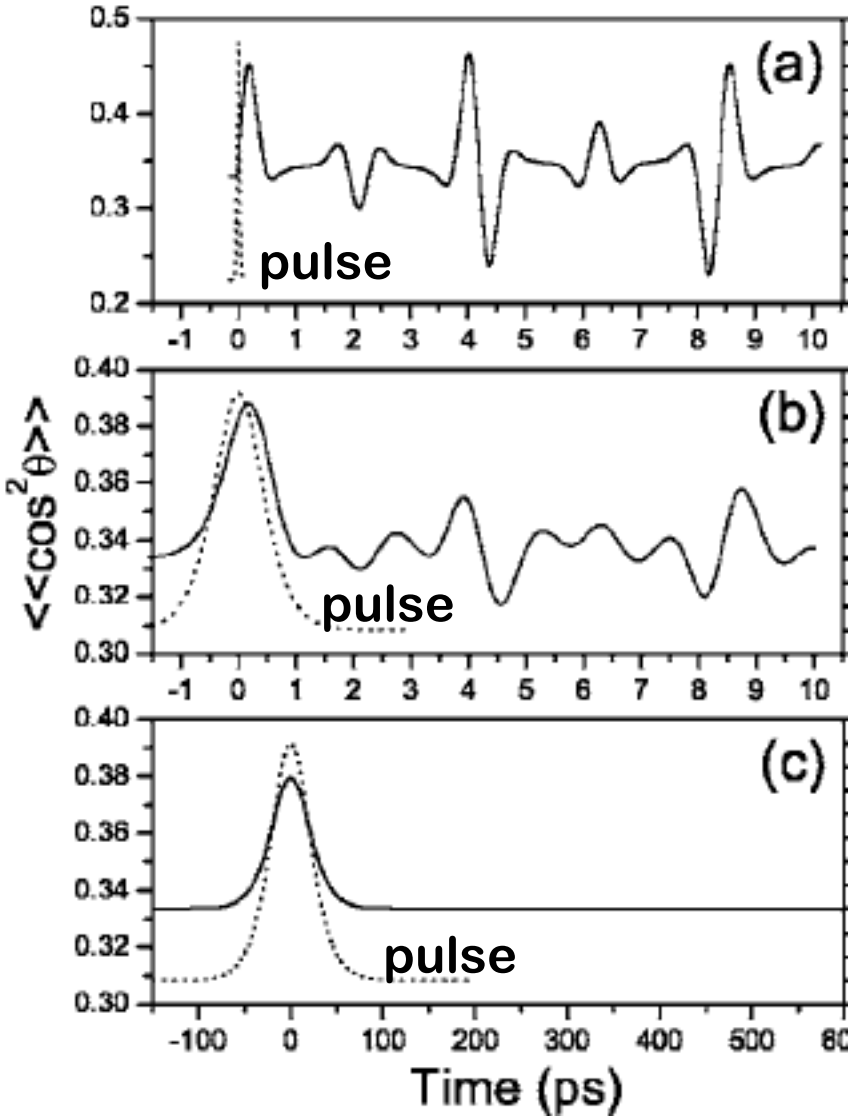

Pulse length 50 fs.

Intensity $2.5 \times 10^{13} \frac{\mathrm{W}}{\mathrm{cm}^2}$.

Impulse regime.

Torres et al., PRA 72, 023420 (2005)

Alignment signal of 1/3 = spherically symmetric. "Rotational revivals" require particular phase relation:

$E_J = B_0 J(J+1) - D_0 J^2 (J+1)^2$.

Pulse length 50 ps.

Intensity $2.5 \times 10^{12} \frac{\mathrm{W}}{\mathrm{cm}^2}$.

Adiabatic regime.

"Kicking" the $^4He_2$: Pump-Probe Experiments

Entirely new regime:

Recall: $^4He_2$ dimer supports exactly one (extremely weakly-bound) state. State is largely universal.
What happens when one applies short (~310fs), intense (~10^{14}W/cm^2) kick?

Separation of time scales (binding energy of 1mK corresponds to 50ns):
Kick is non-adiabatic (quench); in fact, we can simulate it by a delta-function pulse.

Variety of theory predictions:
Friedrich et al., Collect. Czech. Chem. Commun. 63, 1089 (1998); Nielsen et al., PRL 82, 2844 (1999); Bruch, JCP 112, 9773 (2000).

Theoretical Treatment

Dimer potential $V_{eff,J}(R) = V_{He-He}(R) + \frac{\hbar^2 J(J+1)}{2\mu R^2}$

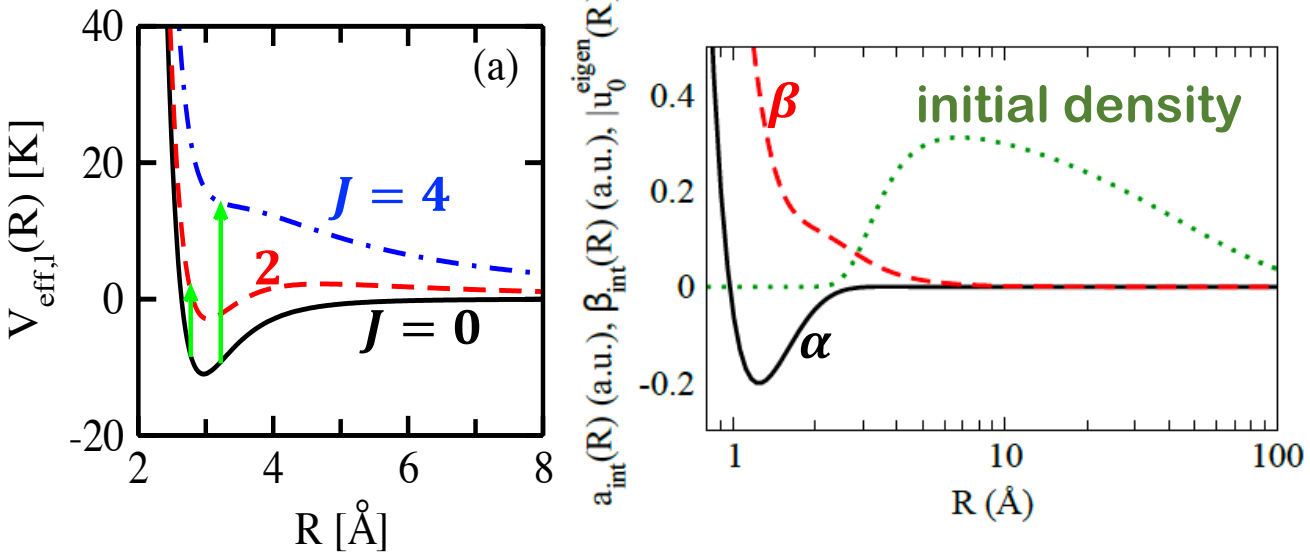

Laser-molecule interaction:

$$V_{lm} = -\frac{1}{2}\varepsilon^2(t)\left[\alpha(R)\, Y_{00}(\hat{R}) + \beta(R)\, Y_{20}(\hat{R})\right]$$

Gaussian profile

Solve time-dependent Schroedinger equation using spherical coordinates:

$$\Psi(R,\theta,t) = \sum_{J=0,2,\ldots} \frac{u_J(R,t)}{R} Y_{J0}(\hat{R})$$

Pulse couples different partial waves.

When pulse is off, the channels are decoupled.

^{4}He-^{4}He In Time-Dependent Electric Field

In what follows, the initial state will be the $J = 0$ eigenstate of the zero-field Hamiltonian of ^{4}He-^{4}He system.

Scenario 1 (non-adiabatic laser kick):

$$\varepsilon(t) = \varepsilon_0 \exp\left(-2\ln 2 \left(\frac{t-t_{ref}}{\tau}\right)^2\right); \tau \approx 300\text{fs}.$$

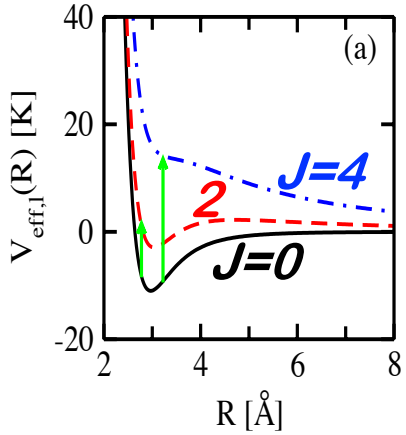

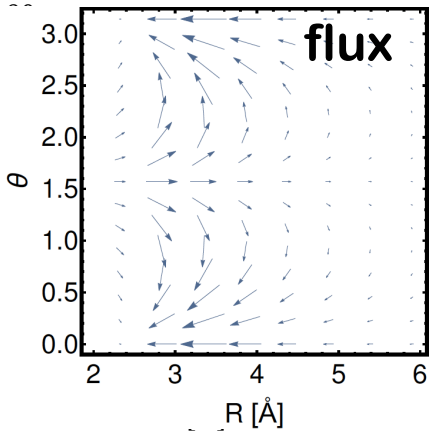

Scenario 2 ("slow"): Gaussian turn-on, hold for several ps, Gaussian turn-off.

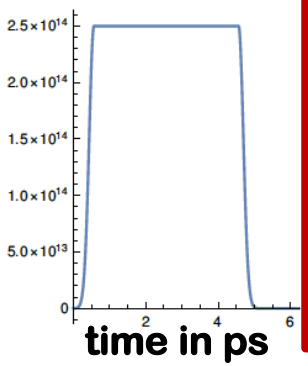

Solve time-dependent Schroedinger equation using spherical coordinates:

$$\Psi(R,\theta,t) = \sum_{J=0,2,\ldots} \frac{u_J(R,t)}{R} Y_{J0}(\hat{R})$$

Laser couples different partial waves.

When laser is off, the channels are decoupled.

Scenario 1: Theory Result

$$C_2(R,t) = \frac{\int_0^\pi \Psi^*(R,\theta,t)\cos^2\theta\Psi(R,\theta,t)\sin\theta d\theta}{\int_0^\pi |\Psi(R,\theta,t)|^2 \sin\theta d\theta}$$

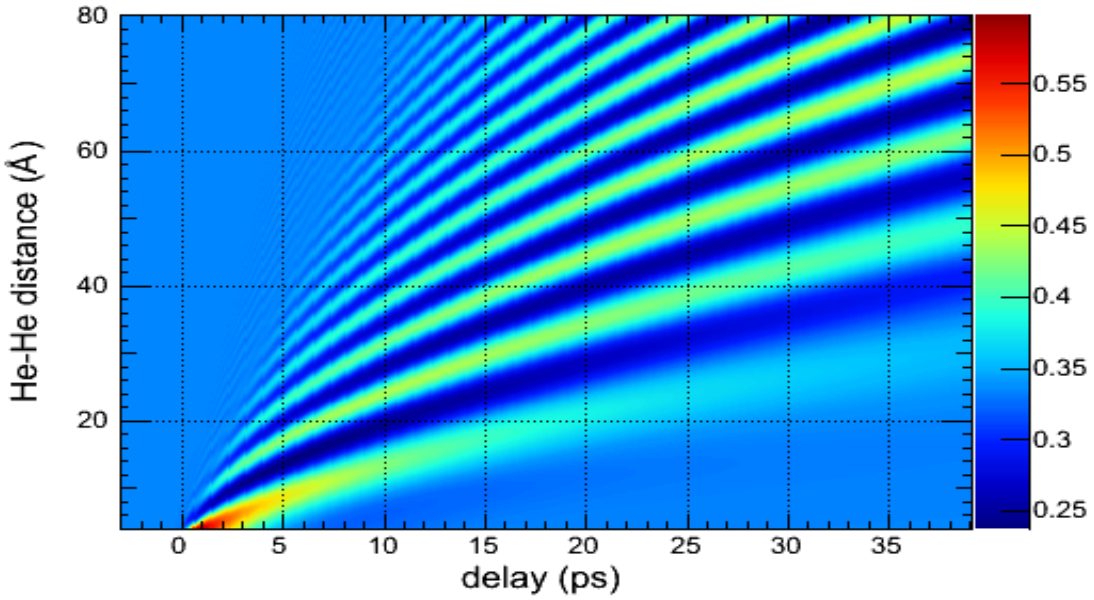

Interference between J=0 and J=2 partial waves. J=2 portion "travels" on structureless background.

Solve time-dependent Schroedinger equation using spherical coordinates:

$$\Psi(R,\theta,t) = \sum_{J=0,2,\ldots} \frac{u_J(R,t)}{R} Y_{J0}(\hat{R})$$

Pulse couples different partial waves.

When pulse is off, the channels are decoupled.

Origin Of The Interference Pattern?

Expand: $\Psi(R,\theta,t) = \sum_{J=0,2,4,\cdots} R^{-1} u_J(R,t) Y_{J0}(\theta)$

$$u_J(R,t) = \exp(\imath\gamma_J(R,t))|u_J(R,t)| \quad \& \quad \tan(\gamma_J(R,t)) = \frac{\mathrm{Im}(u_J(R,t))}{\mathrm{Re}(u_J(R,t))}$$

Plug in:

$$C_2(R,t) = \frac{\int_0^\pi \Psi^*(R,\theta,t)\cos^2\theta\Psi(R,\theta,t)\sin\theta d\theta}{\int_0^\pi |\Psi(R,\theta,t)|^2 \sin\theta d\theta}$$

$$C_2(R,t) = \frac{1}{3} + \frac{4}{3\sqrt{5}}\mathrm{Re}\left(\frac{u_2(R,t)}{u_0(R,t)}\right) + \cdots$$

$$C_2(R,t) = \frac{1}{3} + \frac{4}{3\sqrt{5}}\left|\frac{u_2(R,t)}{u_0(R,t)}\right| \cos(\gamma_2(R,t) - \gamma_0(R,t)) + \cdots$$

Interference Pattern Due To $J = 0$ and $J = 2$ Phases

$$C_2(R,t) = \frac{1}{3} + \frac{4}{3\sqrt{5}} \left| \frac{u_2(R,t)}{u_0(R,t)} \right| \cos(\gamma_2(R,t) - \gamma_0(R,t)) + \cdots$$

Only plotting $J = 0$ and 2

$\gamma_0 \approx const$

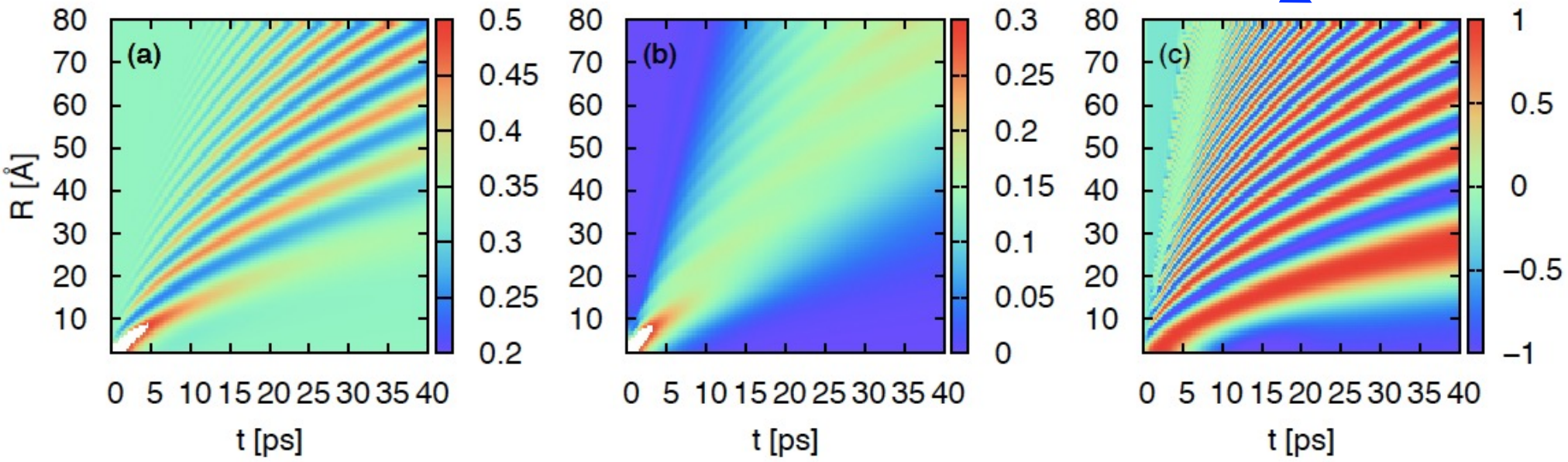

Alignment signal $cos^2\theta$ can be interpreted as measuring $\gamma_2(R,t)$.

Comparison With Experiment

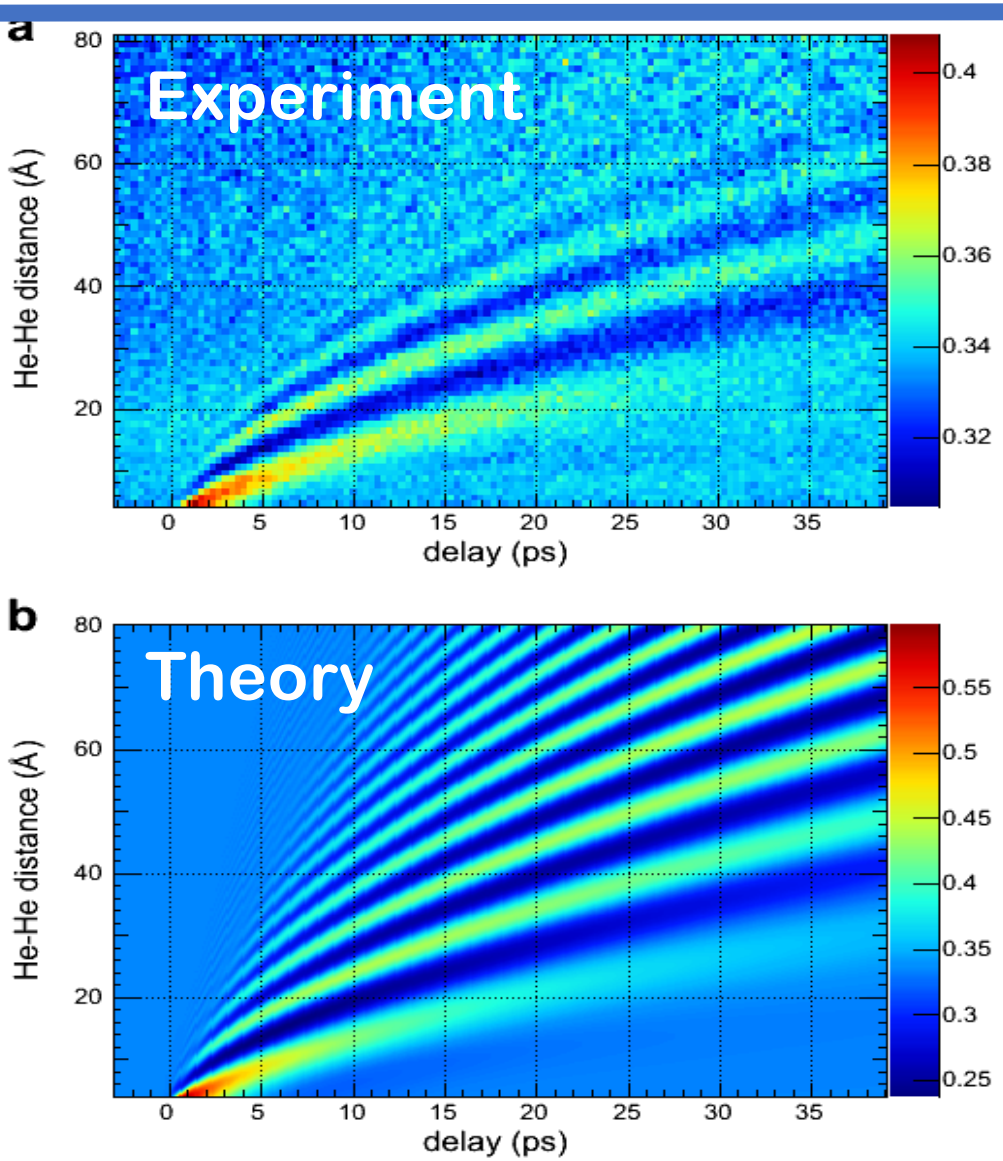

Experimental data by Maksim Kunitski, Reinhard Doerner et al. (Frankfurt University)

Agreement is qualitative but not quantitative.

Need to account for finite experimental resolution.

Experiment

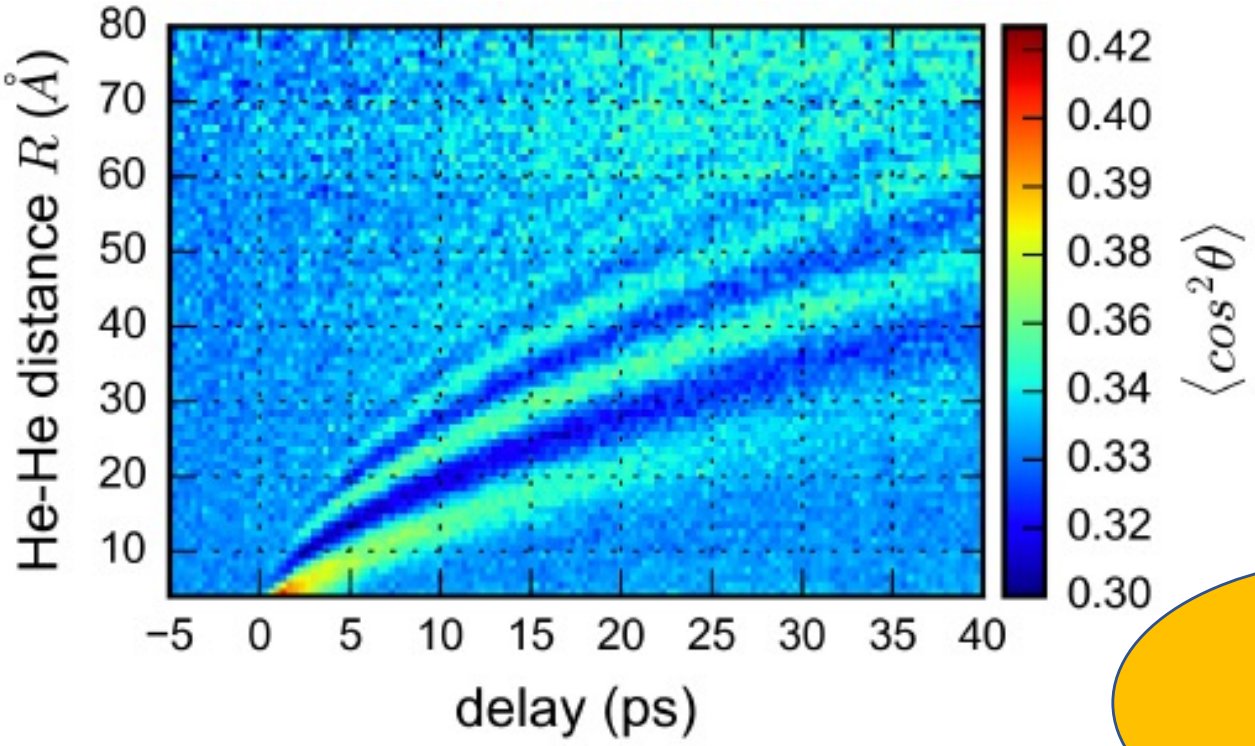

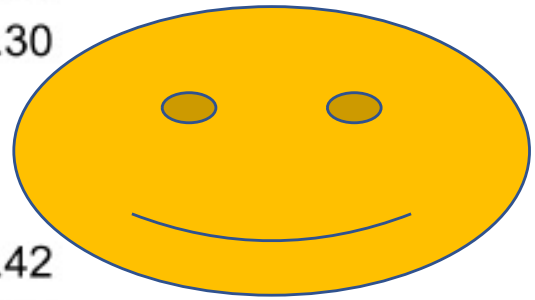

Parameter-free theory (using measured pulse length, intensity, spatial imaging resolution)

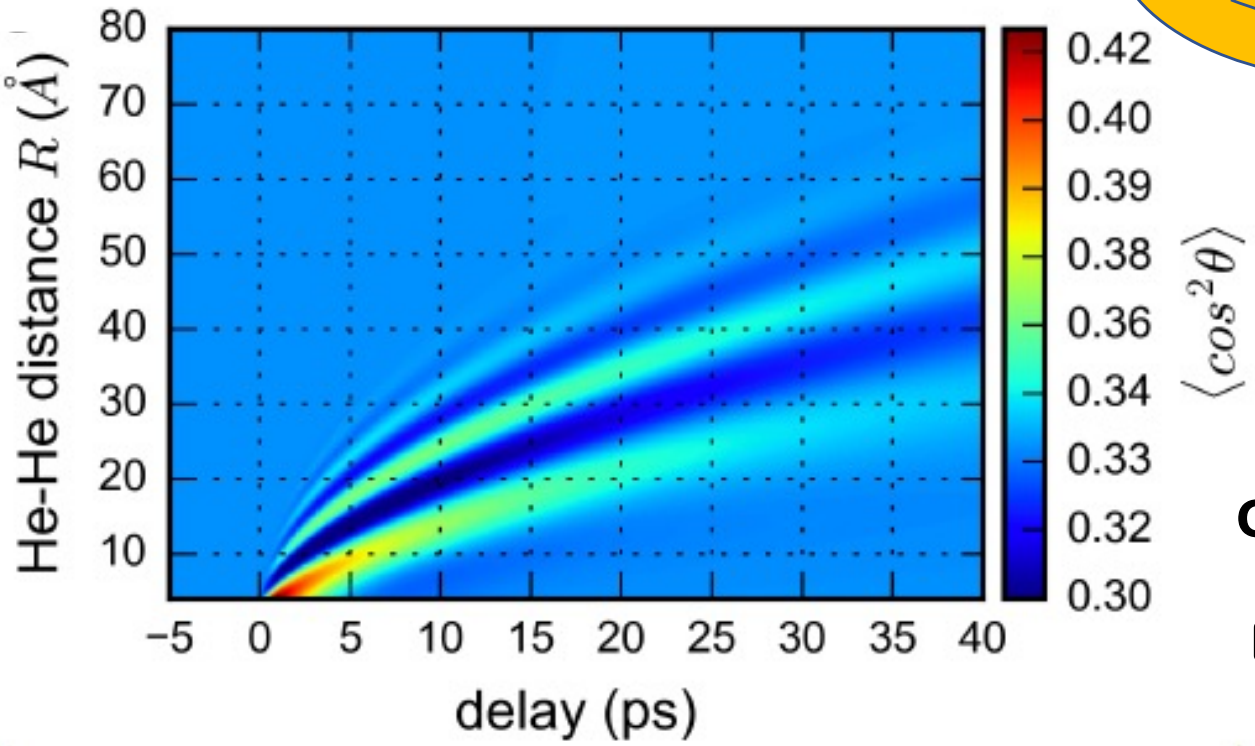

Kunitski, Guan,…,Blume, Doerner, Nature Physics (2021).

Kicking the ^{4}He Dimer

For the first time: Intense laser used to probe dynamics at single-atom level using universal, scattering length dominated initial state.

"Rotationless" ^{4}He dimer can be aligned! Note, it's the continuum portion of the wave packet…

Pattern due to interference between J=0 and J=2 channels: Measurement of spatially and time dependent relative phase between these two partial wave channels. State tomography!

Many outstanding challenges:

Resonances as in ultracold atoms? Need longer pulses…
Time-dependent modulation of interaction strength?
Dynamics of (Efimov) trimers? Need to populate it first…
Larger clusters.

Scenario 2: Longer Pulses

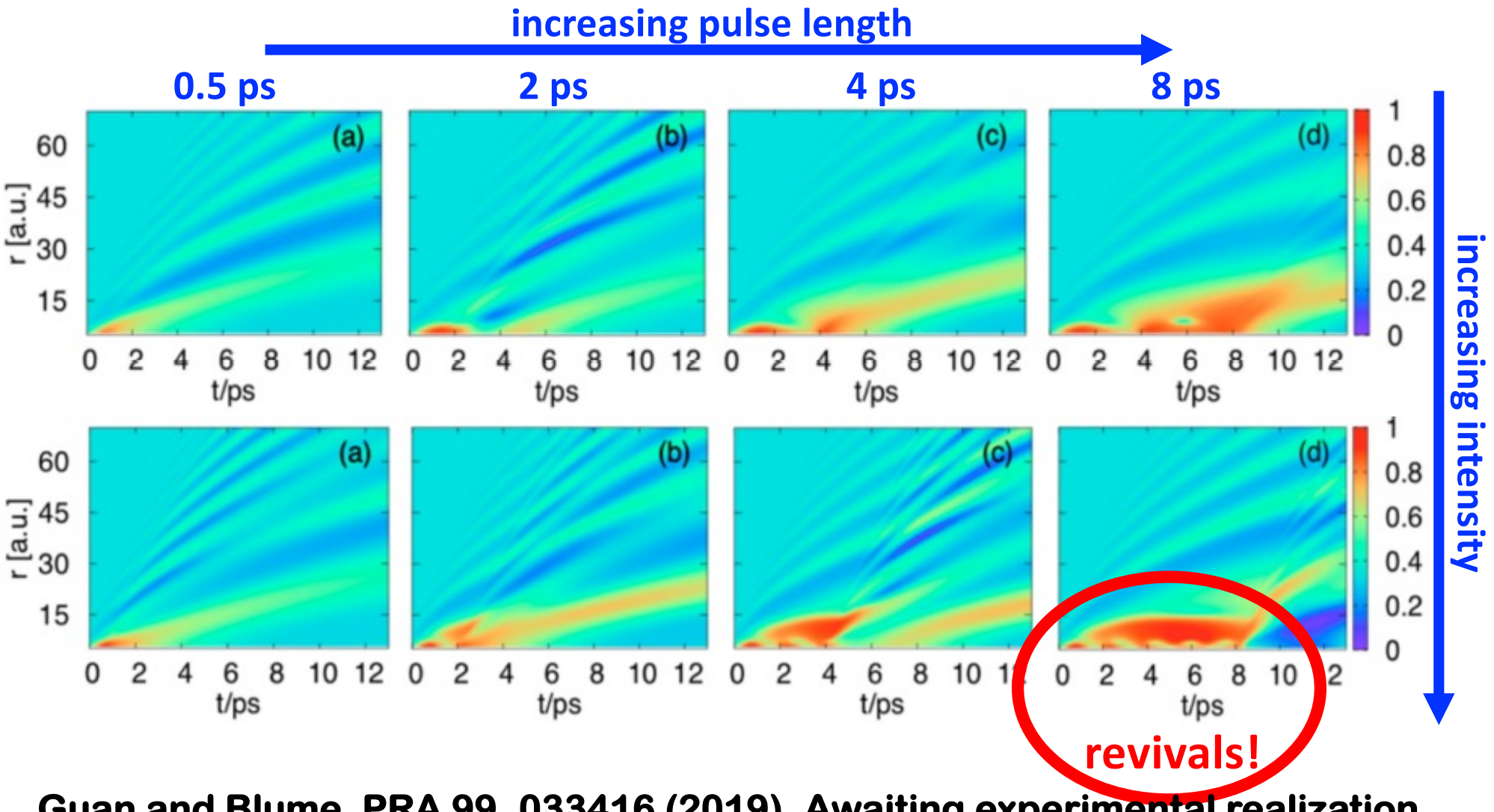

Guan and Blume, PRA 99, 033416 (2019). Awaiting experimental realization…

Signature Of Field-Induced $^4He_2$ Bound States?

$$C_2(R,t) = \frac{\int_0^\pi \Psi^*(R,\theta,t)\cos^2\theta\Psi(R,\theta,t)\sin\theta d\theta}{\int_0^\pi |\Psi(R,\theta,t)|^2\sin\theta d\theta}$$

max. intensity
$2.5 \cdot 10^{14}$ **W/cm²**

4ps hold time

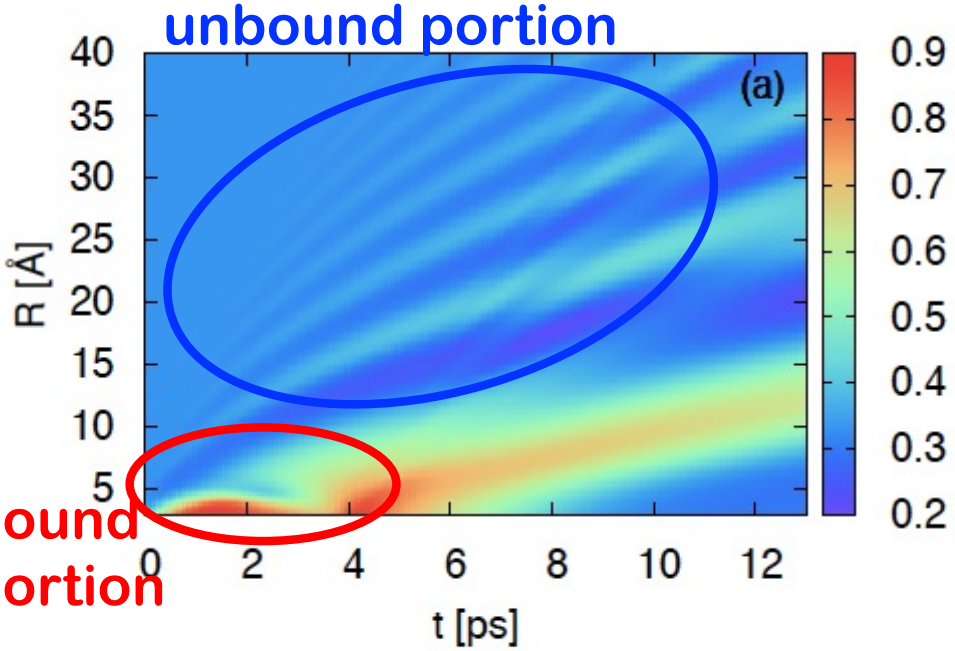

12ps hold time

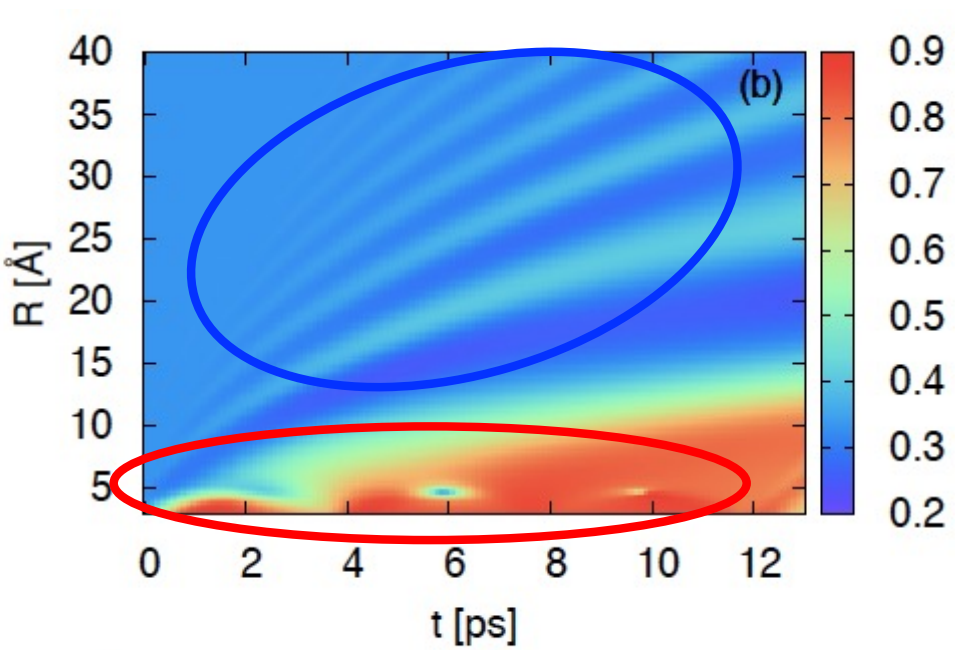

Fingerprint of revivals in time-dependent response of system: Dimer oscillates between deeply-bound state and weakly-bound state.

Summary

- ^4He_N droplets can be realized experimentally in size-selective manner.
- Access to structural properties (accessing real-space structures beyond N=3 is non-trivial due to reconstruction algorithm).
- ^4He-^4He well described by effective range theory (two-parameter theory).
- $^4He_3$: Ground state has Efimov characteristics and excited state is Efimov trimer (s-wave scattering length and three-body parameter).

- If we want more "info," what can be done?
  - Spectroscopy (need more than one bound energy level).
  - Isotope substitution ($^4He \rightarrow {}^3He$).
  - Tuning of interactions (this talk: ground state droplets).
  - Dynamics (this talk: dimer).

Thank You!